

The Pennsylvania State University
The Graduate School
Department of Materials Science and Engineering

**SYNTHESIS AND CHARACTERIZATION OF NOVEL POLYPROPYLENE
SYSTEMS FOR HIGH ENERGY STORAGE CAPACITOR APPLICATIONS**

A Thesis in
Materials Science and Engineering

by
Yuichi Matsuyama

© 2009 Yuichi Matsuyama

Submitted in Partial Fulfillment
of the Requirements
for the Degree of

Master of Science

August 2009

The thesis of Yuichi Matsuyama was reviewed and approved* by the following:

Tze-Chiang Chung
Professor of Materials Science and Engineering
Thesis Advisor

Coray M. Colina
Associate Professor of Materials Science and Engineering
Co-Director The Center for the Study of Polymeric Systems

Ronald Hedden
Assistant Professor of Materials Science and Engineering

Gary L. Messing
Distinguished Professor of Ceramic Science and Engineering
Head of the Department of Materials Science and Engineering

*Signatures are on file in the Graduate School

ABSTRACT

High breakdown strength and high permittivity are two essential properties in a film capacitor for high energy storage applications. Polypropylene is a leading material in this area with a high breakdown strength (>640 MV/m) and a low energy loss (Dissipation factor at 1 kHz, <0.02)¹. However, its low melt strength limits the choice of thermal processing techniques. The melt strength can be improved by the introduction of long chain branches via a synthetic approach using a T-reagent. In this study, the efficiency of a T-reagent was improved through a low temperature (below 37 °C) reaction and a synthesis of a long chain branched polymer containing polyethylene backbone and polypropylene branches (PE-BSt-PP). The low temperature reactions showed improvement in the branch/pendant styrene ratios, and the PE-BSt-PP approach utilized all of the T-reagent present.

Comparisons of linear and branched polypropylene exhibited a reduction in fatal defects in long chain branched polypropylene and increase in the overall stability of the film, indicated by the increases in Weibull alpha and beta values.

Hydroxylation improved the permittivity of polypropylene by a factor of 2 and non-polar polybutadiene by a factor of 10. Compared to the unmodified 1,4-polybutadiene, the dielectric constant of the hydroxylated 1,4-polybutadiene containing alternative vinyl alcohol and ethylene units in the backbone was increased by nearly an order of magnitude at 50 °C and 20 to 200 Hz, due to parallel OH dipole orientation. Investigation of different polymers with various concentrations of hydroxyl groups revealed the correlations between the dielectric constant, concentration of hydroxyl group, structure, and glass transition temperature.

TABLE OF CONTENTS

LIST OF FIGURES	vi
LIST OF TABLES.....	viii
ACKNOWLEDGMENTS	ix
Chapter 1 Introduction	1
1.1 Introduction.....	1
1.2 Long Chain Branched Polymers	3
1.3 Synthesis of Long Chain Branched Polyethylene	5
1.4 Synthesis of Long Chain Branched Polypropylene.....	8
1.4.1 Post-polymerization Modification.....	9
1.4.2 Copolymerization with Non-conjugated Dienes	11
1.4.3 Copolymerization with Butylstyrene or T-reagent.....	13
1.5 Dielectric Properties of Polymer-based Thin Film Capacitors	16
1.5.1 Energy Density	17
1.5.2 Breakdown Strength.....	18
1.5.3 Permittivity.....	20
1.5.4 Polarization-depolarization Loop.....	21
1.6 Polypropylene-based Capacitors	22
1.7 Conclusions.....	23
References.....	25
Chapter 2 Metallocene-mediated Synthesis of Long Chain Branched Polymer Containing Polyethylene and Polypropylene Using T-reagent.....	27
2.1 Introduction.....	27
2.2 Experiment.....	28
2.2.1 Materials and Instrumentation.....	28
2.2.2 Synthesis of Long Chain Branched Polypropylene via T-reagent	29
2.2.3 Copolymerization of Ethylene and P-(3-butenyl)styrene.....	30
2.2.4 Synthesis of LCB Polymers with PE Backbone and PP Side Chains	30
2.3 Branching Efficiency in Metallocene-mediated Synthesis of LCB PP Using T- reagent	30
2.4 New LCB Polymers Having PE Backbone and PP Side Chains.....	36
2.4.1 PE-BSt Copolymers Having LCB Structures.....	37
2.4.2 LCB Polymers with PE Backbone and PP Side Chains (PE-BSt-PP).....	41
2.5 Breakdown Strength of Linear and Branched Polymers	45
2.6 Conclusions.....	47
References.....	49

Chapter 3 Functional Polyolefin-based Capacitors for Energy Storage	50
3.1 Introduction	50
3.2 Experiment	52
3.2.1 Materials and Instrumentation	52
3.2.2 Copolymerization of Propylene and Hexenyl-9-BBN	54
3.2.3 Oxidation Reaction of Polypropylene-butyl-9-BBN Copolymers	54
3.2.4 Functionalization of 1,4-Polybutadiene	55
3.2.5 Thin Film Preparation	55
3.3 Hydroxylated Polypropylene (PP-OH) Dielectric Properties	56
3.3.1 Dielectric Constant of PP-OH Polymers	57
3.3.2 Polarization Loops of PP-OH Polymers	59
3.4 Hydroxylated Polymer Dielectric Spectroscopy	61
3.4.1 Dielectric Constant of Hydroxylated Polymers	62
3.4.2 Polarization-depolarization Curves of Hydroxylated Polymers	71
3.5 Conclusions	74
References	76
Chapter 4 Conclusions and Suggestions	77
4.1 Summary of Present Work	77
4.2 Suggestion for Future Work	79
4.2.1 One-pot Synthesis of Long Chain Branched Structure with PE Backbone and PP Branches	79
4.2.2 Hydroxylation of Non-polar Polymers	80
4.2.2.1 Structural Effect on the Dielectric Constant of Functionalized Polyolefin	80
4.2.2.2 Film Stability and Polarization Curves of Hydroxylated Polymers	81
4.2.2.3 Functionalization with Other Polar Groups	81
References	82

LIST OF FIGURES

Figure 1-1: Power density vs. energy density for various energy storage components.	3
Figure 1-2: Representative linear, branched and crosslinked structures.	4
Figure 1-3: Schemes for the preparation of various linear and branched polyethylene.	6
Figure 1-4: Scheme for the preparation of LCB PE via macromonomer insertion using CGC catalyst.	7
Figure 1-5: Dynamic viscosity vs shear rate measured at 190 °C. LCB densities were 0, 0.22, 0.40 and 0.44 branch per 10,000 carbons.	8
Figure 1-6: Schematic drawing of olefinic terminal groups in polypropylene.	9
Figure 1-7: Scheme of possible consequential branch formation and β -scission in reactive extrusion.	10
Figure 1-8: Scheme for the formation of LCB PP via reactive extrusion in the presence of a sulfide compound and polyfunctional triacrylate.	11
Figure 1-9: Reaction scheme of LCB PP formation via copolymerization with 1,9- decadiene.	12
Figure 1-10: Reaction scheme of LCB PP synthesis via T-reagent.	14
Figure 1-11: Extensional stress growth function at various strain rates for LCB PP at 180 °C.	15
Figure 1-12: Capacitor schematic diagram.	16
Figure 1-13: Setup diagram of electrostatic breakdown strength measurement.	19
Figure 1-14: Representative polarization curves of PP and PVDF. ² U_e is the energy recovered. Areas inside the loops are energy loss.	22
Figure 2-1: Representative ¹ H NMR spectrum of LCB PP.	32
Figure 2-2: LCB/styrene ratio vs temperature plot. Details of each series are in Table 2-1.	33
Figure 2-3: Schematic of the two possible structures produced in a copolymerization of ethylene and butyl styrene. Reaction with the presence of hydrogen produces branched PE-BSt. Reaction without hydrogen produces pseudo-crosslinked PE-BSt. ...	40

Figure 2-4: ^1H NMR spectra of PE-BSt and PE-BSt-PP with different pending styrene consumptions. (a) PE-BSt, (b) PE-BSt-PP 1 with 77 %, and (c) PE-BSt-PP 2 with 100 % consumption.....	43
Figure 2-5: Melting temperatures (T_m) of PE-BSt and PE-BSt-PP samples.....	45
Figure 2-6: Weibull plots of EM, HMS and LCB breakdown strengths measured at room temperature.....	46
Figure 3-1: Dielectric constant of BOPP and PP-OH at 2 kHz.....	57
Figure 3-2: Polarization-depolarization curves of PP-OH and non-functionalized polypropylene derivatives: (a) PP-OH 3, 22 μm , (b) PP-OH 1, 17 μm , and (c) PP-OH 2, 13 μm	60
Figure 3-3: Schematic drawing of polybutadiene, polybutadiene-OH, poly(vinyl alcohol-co-ethylene), and polyvinyl alcohol.....	62
Figure 3-4: Dielectric constant vs temperature spectra of (a) polybutadiene, (b) PB-OH 50, (c) PB-OH 75, and (d) PB-OH 100.....	65
Figure 3-5: Dielectric constant vs temperature spectra of (a) PVA 56, (b) PVA 62, (c) PVA 88, and (d) PVA 99.....	67
Figure 3-6: Dielectric constant vs temperature spectra of (a) PB-OH 75, (b) PB-OH 100, (c) PVA 56, and (d) PVA 99 in heating-cooling scans at 2 kHz. The red triangles represent the heating scan and the blue squares represent the cooling scan.	70
Figure 3-7: Polarization-depolarization curves of (a) PB-OH 100, 17 μm , (b) PVA 56, 17 μm , (c) PVA 62, 16 μm , and (d) PVA 88, 17 μm . Measured at room temperature.....	72

LIST OF TABLES

Table 2-1: Summary of LCB PP polymers prepared by $\text{rac-Me}_2\text{Si}[2\text{-Me-4-Ph(Ind)}]_2\text{ZrCl}_2/\text{MAO}$ mediated bulk polymerizations.	34
Table 2-2: Summary of PE-BSt copolymers by $\text{rac-Me}_2\text{Si}[2\text{-Me-4-Ph(Ind)}]_2\text{ZrCl}_2/\text{MAO}$ mediated in solution polymerizations.	39
Table 2-3: Summary of PE-BSt and propylene copolymerizations.	44
Table 2-4: Breakdown strength analysis of different linear and branched polypropylene using Weibull analysis.	46
Table 3-1: Comparison of hydroxylated polypropylene with various OH concentrations.	57
Table 3-2: Theoretically estimated energy density of BOPP and PP-OH.	58
Table 3-3: General compositions and properties of PB-OH and PVA polymers.	63
Table 3-4: Theoretically estimated energy density of polybutadiene and PB-OH samples at 20 Hz.	69

ACKNOWLEDGMENTS

I would like to use this opportunity to acknowledge many individuals and groups who provided me professional or personal support during my study here at Penn State. I would like to thank Justin Langston and Kevin Masser for their help in different instrumental techniques and many interesting conversations on miscellaneous topics. I would like to thank all my lab mates within the Chung group, particularly Shangtao Chen, who also was an office mate, for the useful tips in syntheses and many interesting conversations on non-research related topics. I also would like to thank Jeff Long at Materials Research Laboratory for the various help with polarization and dielectric constant measurements. I would like to acknowledge my friends for their miscellaneous supports, and the staff and faculty members in Steidle for their help in making my studies at Penn State go smoothly. I would like to thank all my committee members for their attention despite my many grammatical and spelling mistakes. A special thanks goes to Professor Ronald Hedden for providing me with much useful input on various issues. A special thanks goes to my thesis adviser, Professor Mike Chung, who provided me with advice, guideline, and support during my study at Penn State. His professional research know-how was the most variable knowledge I gained from Dr. Chung. Finally, a special thanks goes to my family. Their encouragement and support greatly helped during my graduate study.

Chapter 1

Introduction

1.1 Introduction

This is the century of energy storage – this statement is by no means an exaggeration. With rapid advancement of technologies in the ‘90s, every electronic device became more sophisticated; some became smaller while some others became multi-functional. These improvements, however, also raised energy storage issues. One simple example is a cell phone, which has now become an essential item in modern life. In addition to its high possession rates, the capabilities of an individual device dramatically improved, allowing it to become something more than a telephone. Important questions that need to be pondered are: How can sufficient energy be stored to operate cell phones and many other devices with multi-functionalities? How efficiently can we store energy for different applications? There have been intense studies on energy storage issues at the governmental, academic and industrial scales.

Film capacitors are one energy storage device which have received increasing attention in recent years. Historically, batteries have been the dominant energy storage device as they have high energy density and the stored energy can be slowly released for use as needed. Thus, batteries have widely been used in portable electronic devices. Film capacitors have a much lower energy density than batteries, super capacitors or electrolytic capacitors, as depicted in Figure 1-1.³ Unlike batteries, the stored energy in a capacitor cannot be used in a gradual manner; instead all the energy is instantaneously discharged upon use which provides a high power density. Despite its low energy density, the superiority of its power density makes a capacitor favorable in applications such as automobile engine ignition and the phase-lock loop used in cell phones.⁴

Although they are already being used in hybrid cars and power electronics circuits in Shinkansen bullet trains⁵, improvement in the energy density of solid-state capacitors is highly desired. This can be accomplished by the development of materials with high processibility and suitable behavior under an electric field.

Among various candidate dielectric materials for capacitors, polymer films are highly favorable due to their flexibility, processibility, light weight and cost. As will be discussed in Section 1.4, a film capacitor stores energy on its surface. It is thus important that the film thickness is reduced to achieve the highest energy density per volume. At the same time high film quality is crucial, as defects dramatically reduce the breakdown strength or resistivity against an electric field. Currently, commercial thin polypropylene capacitor films are produced via thermal extrusion followed by biaxial stretching. In these processes, there are several key factors: the polymer needs to have high melt strength and thermal processibility, and the processed film needs to be void free. However, isotactic polypropylene synthesized by metallocene catalyst typically has a narrow molecular weight distribution and low melt strength. One solution is the incorporation of long chain branches, which improves the thermal processibility of a polymer and enables the preparation of a high-quality film with minimal defects.

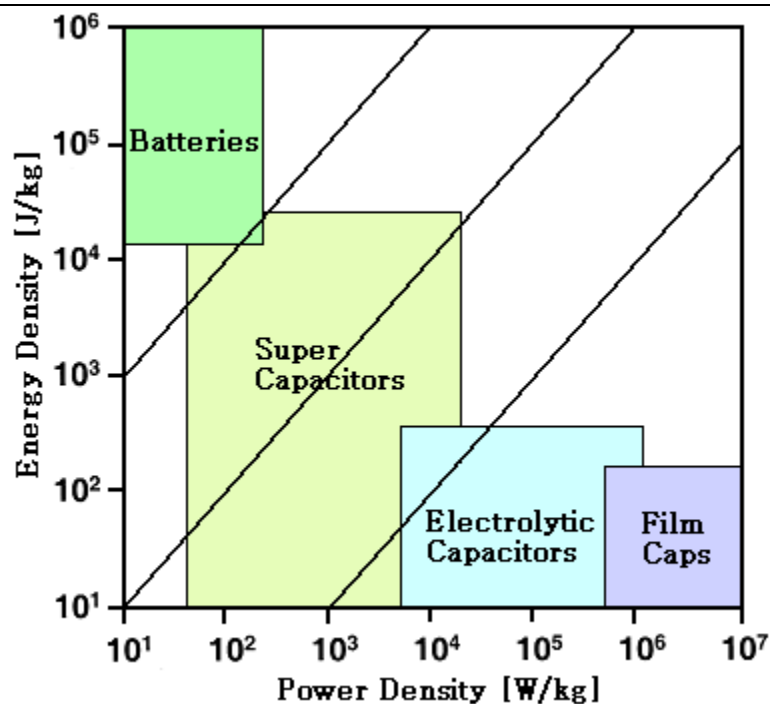


Figure 1-1: Power density vs. energy density for various energy storage components.³

1.2 Long Chain Branched Polymers

Polymeric materials have become popular particularly in the last few decades, and they have been replacing metals, ceramics, and other materials that have traditionally been used in various applications. For example, crosslinked polymeric fillings are now commonly used by dentists in place of silver amalgam for better appearance and stability.⁶ Another example is Boeing's 787 Dreamliner, which will use a carbon-fiber composite in half of its body for an improved fuel efficiency.⁷ The major advantage of a polymeric system is its flexibility, which enables a structure to be custom-tailored by varying the combination of constituent repeating units and their arrangements. Polymer structures can generally be categorized into three types: linear (one dimensional), branched (two dimensional), or crosslinked (three dimensional) (Figure

1-2). The most common of the three architectures is linear, and some examples include polystyrene and polyisoprene. Branched or crosslinked polymers differ from linear polymers in their properties and processibility, which increases the possible number of applications. In fact, long chain branched polymers are suitable in processing techniques where high melt strength is demanded, such as film blowing, thermoforming and extrusion coating.

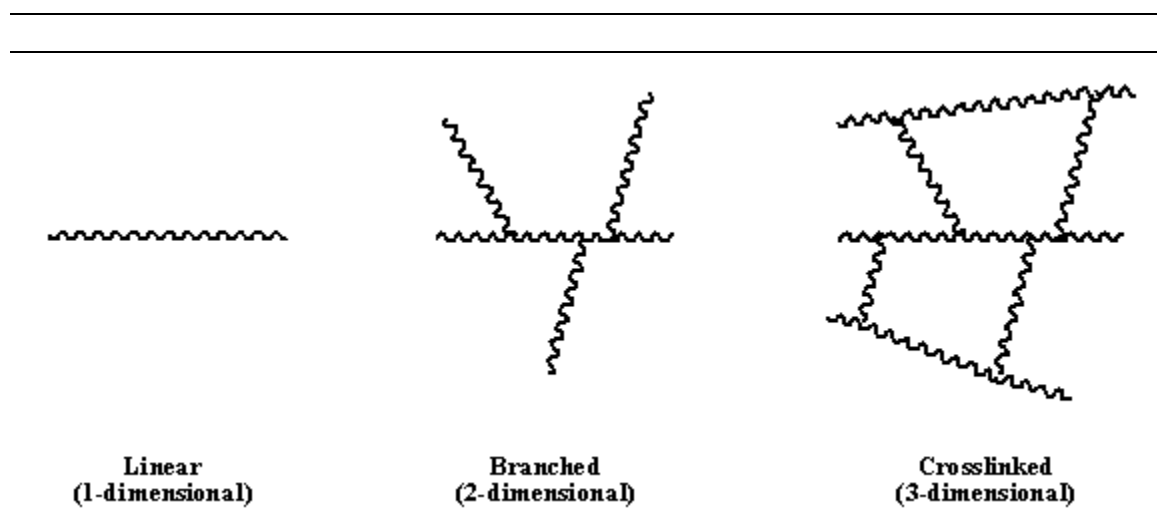


Figure 1-2: Representative linear, branched and crosslinked structures.

Long chain branched polyethylene (LCB PE) is a representative example of a successful commercial branched polymer. The wide choices of synthetic routes and types of branching in LCB PE production have made it a commercially popular processing material. Despite its structural similarity to polyethylene, and its better thermal and mechanical properties, polypropylene has not gained much attention primarily due to the limited chemistry available to produce highly isotactic polypropylene. Isotactic polypropylene is generally synthesized via Ziegler-Natta or metallocene catalysts. These catalysts, however, are sensitive to functional comonomers and generally do not produce a branched structure.⁸ Alternative approaches have been employed by different groups, including electron beam irradiation, reactive extrusion, and

copolymerization with dienes. These methods produced long chain branched polypropylene, yet there were some drawbacks in the structures of the products, as will be discussed in Section 1.4.

1.3 Synthesis of Long Chain Branched Polyethylene

Polyethylene, a polymer with a simple $-\text{CH}_2-\text{CH}_2-$ repeating unit, can be classified into four groups depending on the structure: a linear structure known as high density polyethylene (HDPE), a structure with numerous short branches known as linear low density polyethylene (LLDPE), a polymer chain with a mixture of short and long branches referred to as low density polyethylene (LDPE), and long chain branched polyethylene (LCB PE). Brief chemical equations are shown in Figure 1-3.

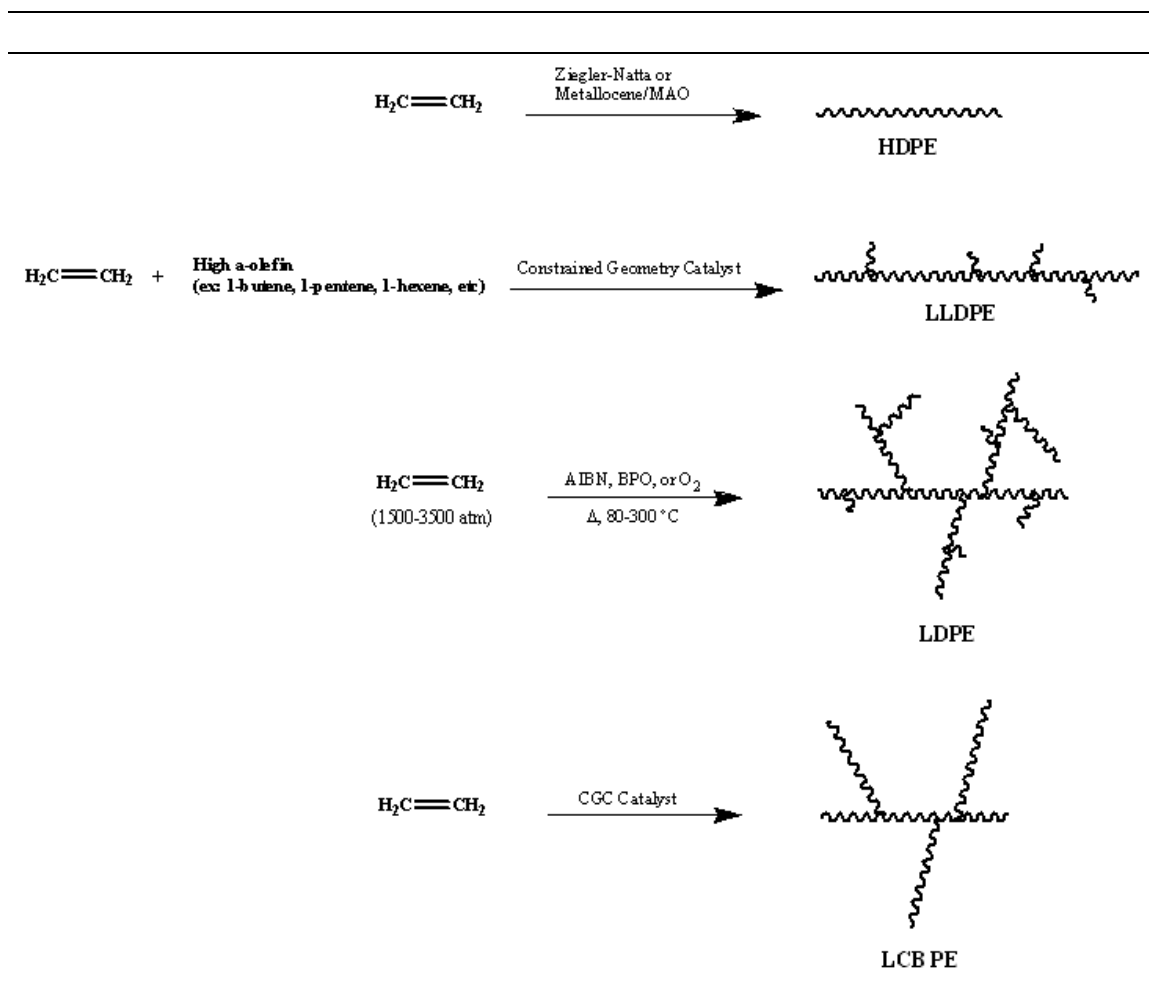


Figure 1-3: Schemes for the preparation of various linear and branched polyethylene.⁹

High density polyethylene or a linear structure is synthesized by the homopolymerization of ethylene using Ziegler-Natta or metallocene/MAO catalyst. Linear low density polyethylene is synthesized by a copolymerization of ethylene and high α -olefin, such as 1-butene, 1-pentene, and 1-hexene, using metallocene, particularly a constrained geometry catalyst (CGC).^{10, 11} As illustrated in Figure 1-3, the product structures are a mixture of short and long branches that are grafted on the backbone and on the other branches. Homopolymerization of ethylene using CGC catalyst produces long chain branched polyethylene.¹¹⁻¹³ Among variations of CGC catalysts, the

Insite CGC catalyst developed by Dow Chemical Company is the one that is most frequently referred to in the synthesis of LCB PE.^{11,14}

The reaction mechanism of long chain branched polyethylene synthesis by CGC catalyst is illustrated in Figure 1-4. The reaction involves the initial formation of a vinyl terminated macromonomer via β -hydride elimination. The vinyl end is then re-incorporated into another polyethylene chain.^{11,14} The produced LCB PE has a narrow molecular weight distribution and enhanced processibility, two properties which would not exist simultaneously in a linear polyethylene produced by a metallocene catalyst.¹⁴ Yan et al.¹² synthesized LCB PE using Dow Chemical's CGC catalyst and reported the experimental results. Comparisons of LCB PE polymers with similar molecular weights but different branch densities showed an enhanced shear thinning, even at an extremely low concentration of branches (Figure 1-5). ¹³C nuclear magnetic resonance spectra supported the presence of branches in the samples.¹² The reported experimental results showed the successful formation of long chain branches, and their effects even at low concentrations.

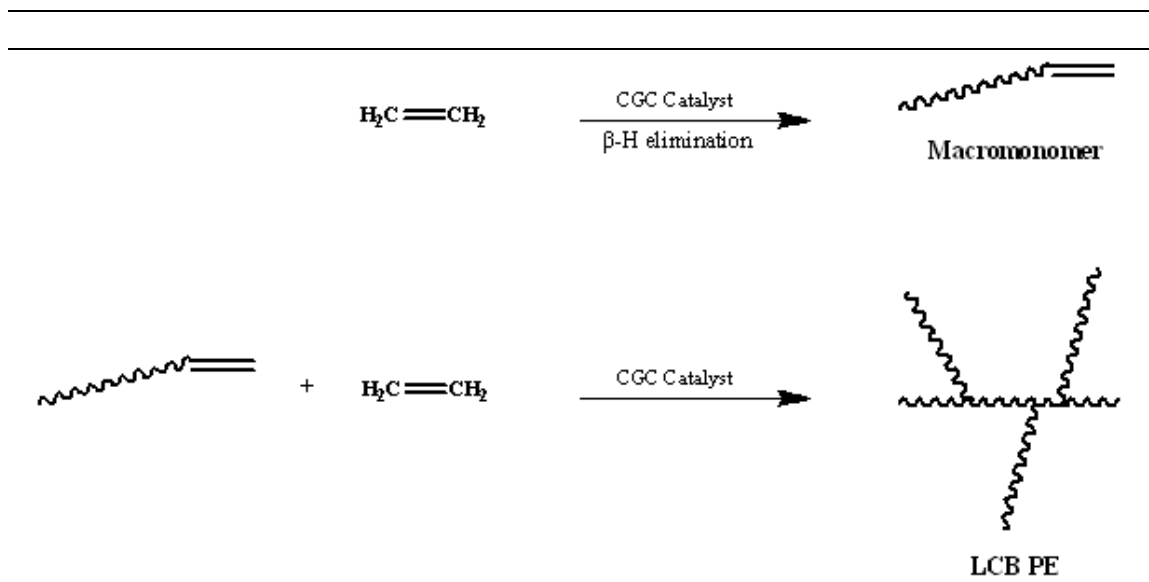


Figure 1-4: Scheme for the preparation of LCB PE via macromonomer insertion using CGC catalyst.

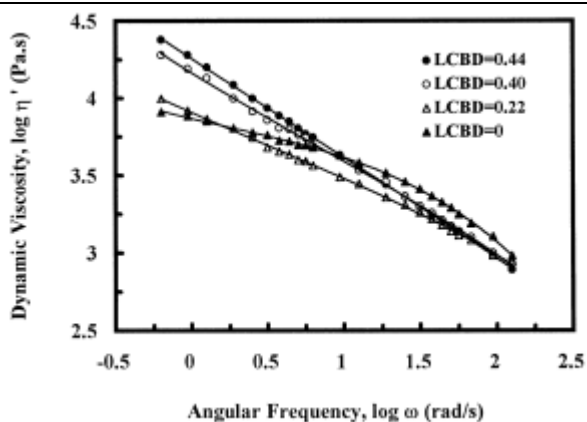


Figure 1-5: Dynamic viscosity vs shear rate measured at 190 °C. LCB densities were 0, 0.22, 0.40 and 0.44 branch per 10,000 carbons.¹²

1.4 Synthesis of Long Chain Branched Polypropylene

Isotactic polypropylene is a widely used commercial polymer with the advantages of good impact strength, high rigidity, good chemical and electrical resistance, and low cost. Despite these beneficial properties and its wide commercial usages, polypropylene has a low melt strength and the processing techniques utilized for polyethylene were traditionally not fully employed for polypropylene.^{8, 15} The melt strength of polyethylene was improved via the incorporation of long chain branches, and the synthetic approaches are detailed in the previous section. These reactions, however, are not directly applicable to polypropylene. While β -hydride elimination is the predominant mechanism for chain termination in metallocene-catalyzed reactions, it does not form vinyl chain ends in most propylene polymerizations.¹⁶ Vinylidene chain ends, most commonly formed in propylene polymerizations, are not as reactive as the vinyl chain ends. As illustrated in Figure 1-6, non-vinyl olefinic chain ends are not openly accessible and they are harder to further incorporate into polypropylene chains. As a result, long chain branched

polypropylene cannot be as readily synthesized as long chain branched polyethylene using Ziegler-Natta or metallocene/MAO catalysts. In spite of the synthetic difficulty, the improved melt strength of a branched polypropylene is highly desirable for thermal processing. For this reason, attempts have been made by various research groups to synthesize a highly isotactic long chain branched polypropylene using alternative approaches. Some examples of the explored methods include post-polymerization modification, copolymerization with non-conjugated dienes, and copolymerization with butyl styrene.^{8, 17-20}

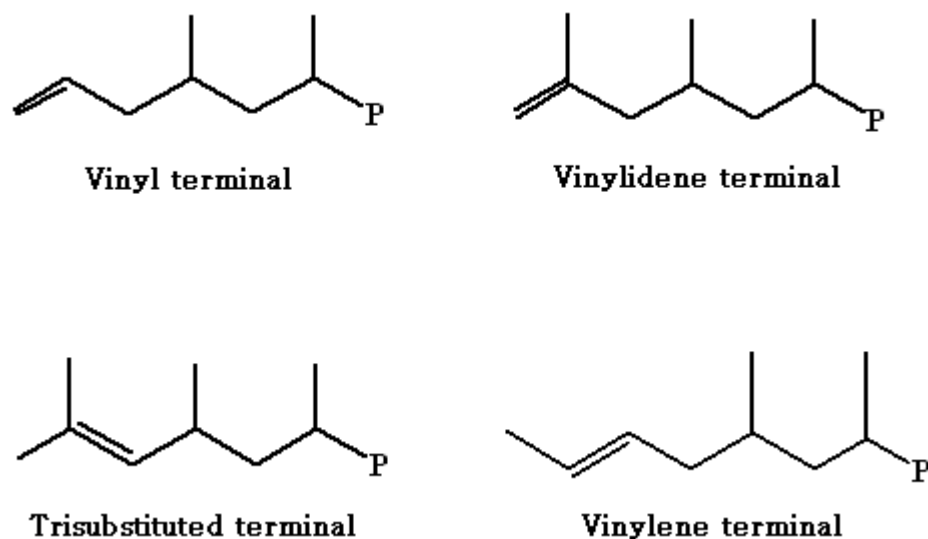


Figure 1-6: Schematic drawing of olefinic terminal groups in polypropylene.¹⁶

1.4.1 Post-polymerization Modification

Electron beam irradiation and reactive extrusion are both post-polymerization modifications. A general reaction scheme for the creation of a branched PP is illustrated in Figure 1-7.

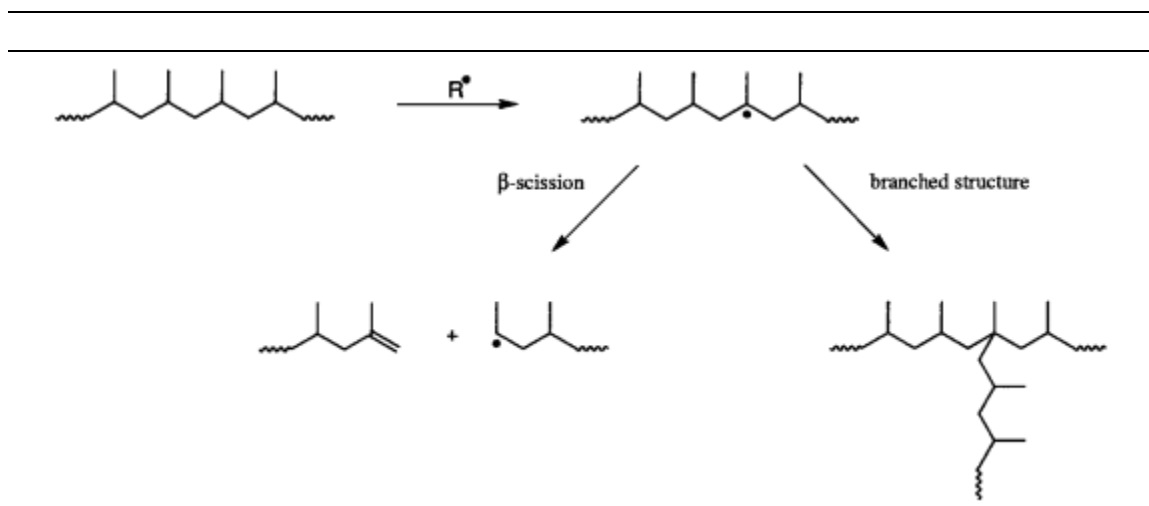


Figure 1-7: Scheme of possible consequential branch formation and β -scission in reactive extrusion.¹⁷

In both modifications, isotactic polypropylene is used as the starting polymer. The employed electron beam or free radicals generated from decomposed peroxide attack the polypropylene chains and abstract the proton on the tertiary carbons.¹⁷⁻¹⁹ The radical possessing polypropylene chain then goes through either further chain cleavage by β -scission or branch formation. These are two competing reactions, and the unstable tertiary radical leads to rapid degradation particularly at high temperatures. The use of relatively low temperature, therefore, is not only important in the control of free radical generation, but also in the reduction in the rate of β -scission, which would reduce the molecular weight of the product.

Graebling¹⁷ reported the stabilization of tertiary radicals and promotion of long chain branch formation using a sulfide compound, such as thiuram disulfide, and a polyfunctional triacrylate. When thermally decomposed, thiuram disulfide produces two dithiocarbamate radicals which readily react with tertiary radicals (Figure 1-8). This reduces the concentration of free radicals, which helps to prevent β -scission. The introduced trimethylol propane triacrylate (TMPTA), a triacrylate monomer, also reacts with tertiary radicals and forms a more stable secondary radical. The created secondary radical of TMPTA-polypropylene and unreacted

tertiary radicals then react to form branches. This method thus reduces β -scission and increases the efficiency of long chain branch formation. Despite these improvements, potential degradation, reduction in the molecular weight, and difficulties in controlling branch structures are major problems in post-polymerization modifications that limit the usage of these LCB PP preparation methods.

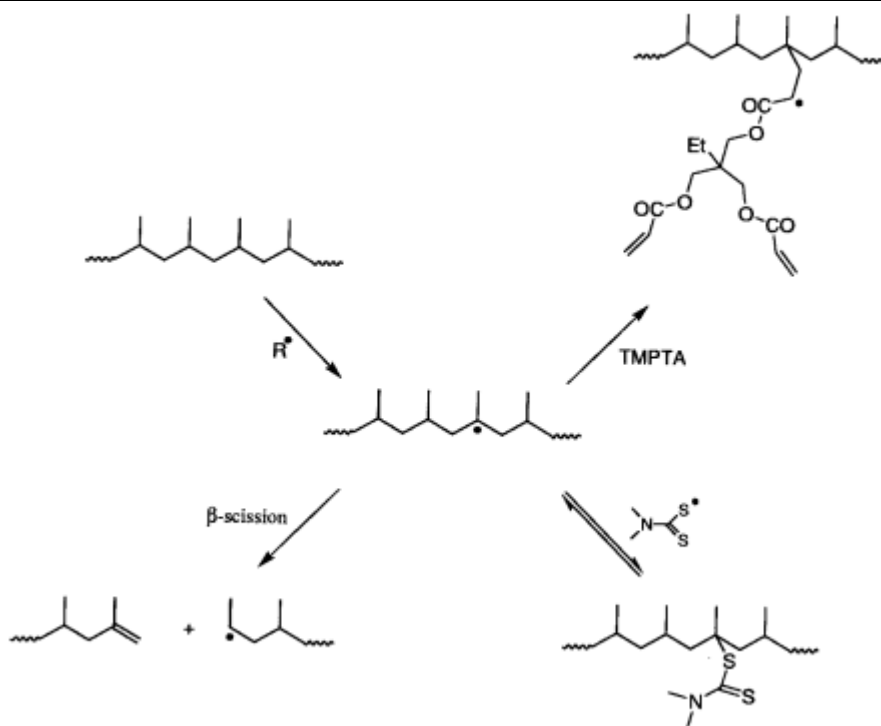


Figure 1-8: Scheme for the formation of LCB PP via reactive extrusion in the presence of a sulfide compound and polyfunctional triacrylate.¹⁷

1.4.2 Copolymerization with Non-conjugated Dienes

Unlike the post-polymerization modification discussed in the previous section, copolymerization with non-conjugated dienes is β -scission free. As illustrated in Figure 1-9, one end of a non-conjugated diene initially copolymerizes and is incorporated into a polypropylene

chain.²⁰ A long chain branch is formed when the terminal diene is incorporated into another polypropylene chain. This in-situ formation of long chain branches during polymerization is suitable for obtaining high molecular weights.

While copolymerization of propylene and non-conjugated dienes produces long chain branched polypropylene without degradation or β -scission, this method has a limitation in the concentration of diene comonomer that can be used in the polymerization reaction. One unique feature of the long chain branches created via this method is the presence of multiple long chain branches within a branch. In other words, the incorporated dienes could link multiple polymer chains and form a structure that resembles a crosslinked polymer. Incorporation of long chain branches improves the melt strength of a polymer and this essentially leads to easier thermal processing, but a highly crosslinked structure greatly limits its processibility. Unfortunately, the degree of crosslinking in the product cannot be controlled. Therefore, the concentration of diene comonomer must be kept very low to prevent possible crosslinking.

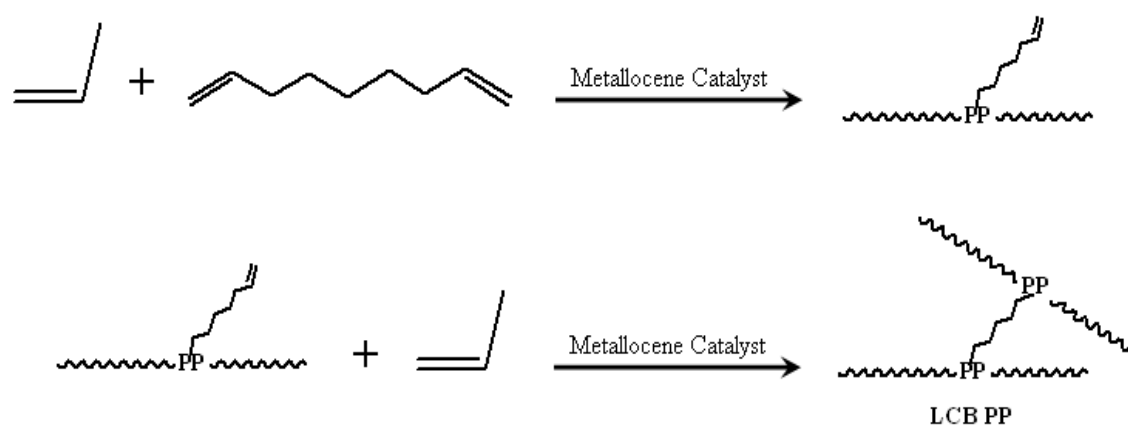


Figure 1-9: Reaction scheme of LCB PP formation via copolymerization with 1,9-decadiene.²⁰

1.4.3 Copolymerization with Butylstyrene or T-reagent

Another approach towards the synthesis of long chain branched polypropylene via copolymerization with butylstyrene (BSt) or T-reagent was developed by the Chung group at Penn State. This reaction involves the incorporation of BSt in the backbone and chain transfer of polypropylene polymer chains to the pendant styrene groups of the incorporated BSt (Figure **1-10**).⁸ The comonomer used in this reaction is also a conjugated diene; however, the difference in the catalyst reactivity to the allyl and styrene ends restricts the formation of a crosslinked structure.

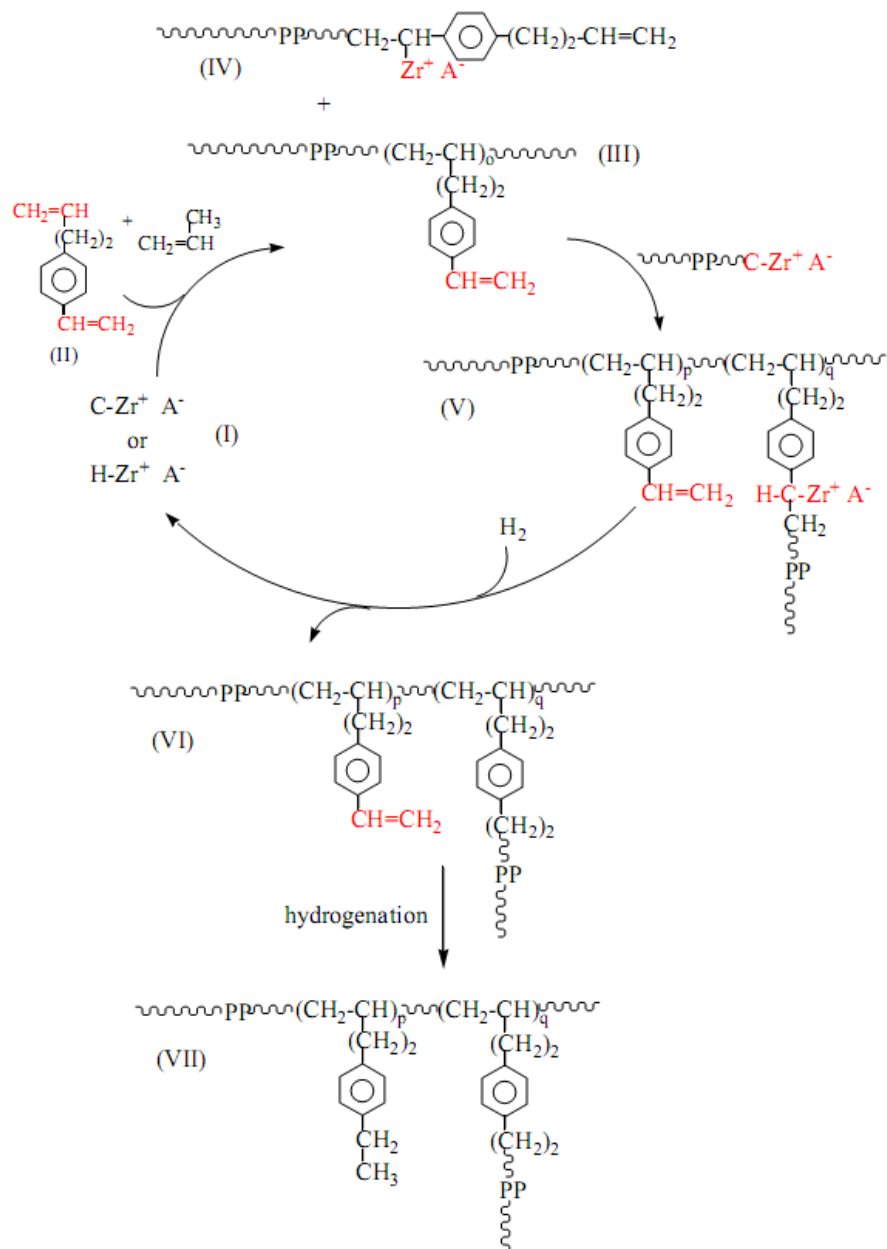


Figure 1-10: Reaction scheme of LCB PP synthesis via T-reagent.⁸

This synthetic method is superior to the other PP methods discussed in the previous sections, as this method is degradation and crosslinking free, and there is no restriction in the product molecular weight or branch density. Langston et al.⁸ evaluated the long chain branch

polypropylene prepared by this method and observed strain hardening of the polymer, a typical behavior of a branched material (Figure 1-11).

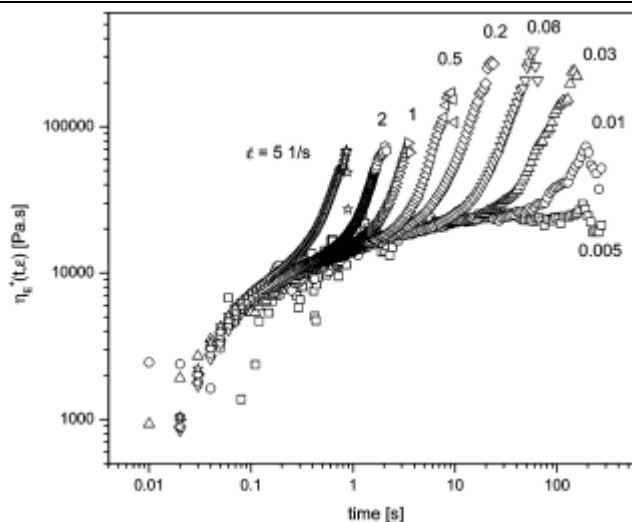


Figure 1-11: Extensional stress growth function at various strain rates for LCB PP at 180 °C. ⁸

One of the areas the long chain branched polypropylene synthesis via BSt is in need of further study is the improvement of T-reagent efficiency, since only 15 to 25 % of BSt is consumed in a typical reaction and 50 % or less of the incorporated BSt constitutes long chain branches. Improved consumption of T-reagent and formation of long chain branches are both desirable for the maximum utilization of the branching reagent. Also, efficient branch formation would help to reduce the concentration of styrene groups of the incorporated BSt. This is important in keeping the polymer processable and more homogeneous as well as in minimizing possible crosslink formation, which can result from dimerization between two pendant styrene units during melt processing. It is, therefore, desirable not only to consume more BSt but also to reduce the styrene concentration.

1.5 Dielectric Properties of Polymer-based Thin Film Capacitors

As previously mentioned in Section 1.1, film capacitors are energy storage devices which specialize in high power storage. Among capacitor candidate dielectric materials, polymer films are becoming more important due to their flexibility, processibility, light weight and cost. It is therefore important to understand the principles of a capacitor to maximize the energy storage capability of a polymer thin film capacitor.

A capacitor stores energy in the form of an electrostatic field by separating charges, and its system setup is simple. (Figure 1-12) When two parallel plates that are connected to an electrical current source, such as a battery, are placed very close together, positive and negative charges accumulate on the surfaces of the plates.²¹ When excess charges are built up on the surfaces, the system discharges by breaking the insulating medium between the plates, neutralizing the charges previously built up on the electrodes. In the example just explained, air was the insulating medium. However, the insulator medium can also be paper, polymers, composites, or many other materials.

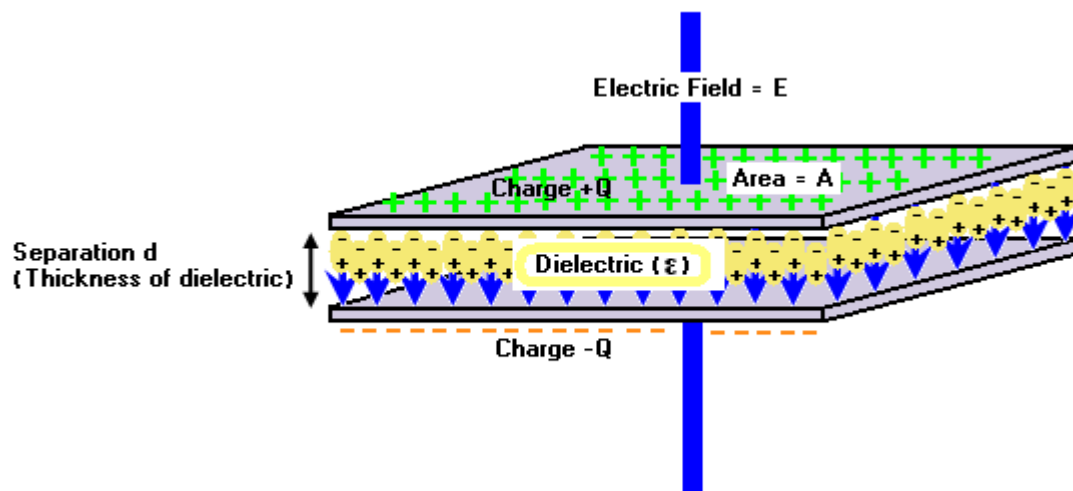


Figure 1-12: Capacitor schematic diagram.²²

In a capacitor, the charges are stored on the surfaces of the material. This implies that a thin film is a desirable form of a capacitor to store the highest energy per volume. This is a rather difficult case for some dielectric materials, such as glasses and ceramics, as their stiffness hinders them from being made into a roll of thin film. On the other hand, polymers such as polypropylene and polyethylene are most suitable for processing into a flexible film. In addition, metalized polymer film capacitors have a self-healing behavior which helps to maintain the overall film quality, while a local failure in a ceramic capacitor causes the whole capacitor system to fail. With these advantages, polymers are a great candidate for a next-generation capacitor with enhanced energy storage.

1.5.1 Energy Density

While the basic principle of a capacitor is simple, energy storage in a capacitor involves many factors that need to be considered. The energy density of a dielectric material can be described as follows²³:

$$U_e = \frac{1}{2}DE$$

where U_e is energy density, D is charge displacement, and E is the magnitude of the electric field. Charge displacement, D , can be expressed as:

$$D = \epsilon\epsilon_0 E$$

where ϵ is dielectric constant, and ϵ_0 is the permittivity of free space, having a value of $8.85 \times 10^{-12} \text{ F/m}$. Also, the electric field can be described as:

$$E = V/d$$

where V is the voltage applied and d is distance between charges or thickness of the insulating medium. Using this information, the energy density equation can be rewritten as:

$$U_e = \frac{1}{2} \epsilon \epsilon_0 E^2 = \frac{1}{2} \epsilon \epsilon_0 \left(\frac{V}{d} \right)^2$$

This equation is used in the energy density calculations, and it also indicates that two approaches are available in increasing the total amount of energy stored. For a given voltage applied and an insulator with dielectric constant ϵ , one can increase the energy density stored by increasing the permittivity of the insulating medium or by decreasing the thickness of the medium.

1.5.2 Breakdown Strength

Electrical breakdown strength of a material is described as the maximum voltage that can be applied per unit thickness. Expressed in the equation, breakdown strength is thickness dependent, and reduction in the thickness proportionally reduces the voltage needed to attain the same breakdown strength. In addition to the film thickness, breakdown strength is greatly influenced by the presence of defects, as current passes through the weakest spot in the film matrix. Common defects include air bubbles, residual solvents and pinholes. The sensitivity of the breakdown strength to these defects is tremendous: Fukuda reported that the vapor curing method in silane-crosslinked polyethylene (XLPE) was troublesome, as the water used in the cooling of XLPE left pathways or voids as it escaped from the film.²⁴ This example shows that minimization of voids is essential in the maximization of breakdown strength.

The breakdown strength of a film is measured by sandwiching the film between two electrodes and ramping up the applied voltage until the film fails. Traditionally gold electrodes have been sputtered on the film, however, commercial metalized polypropylene films have been

more commonly used in recent years to prevent damage to the film and to minimize unevenness of the electrode thickness. In this approach, the sample film and an insulating mask are sandwiched between two metalized films (Figure 1-13)²⁵.

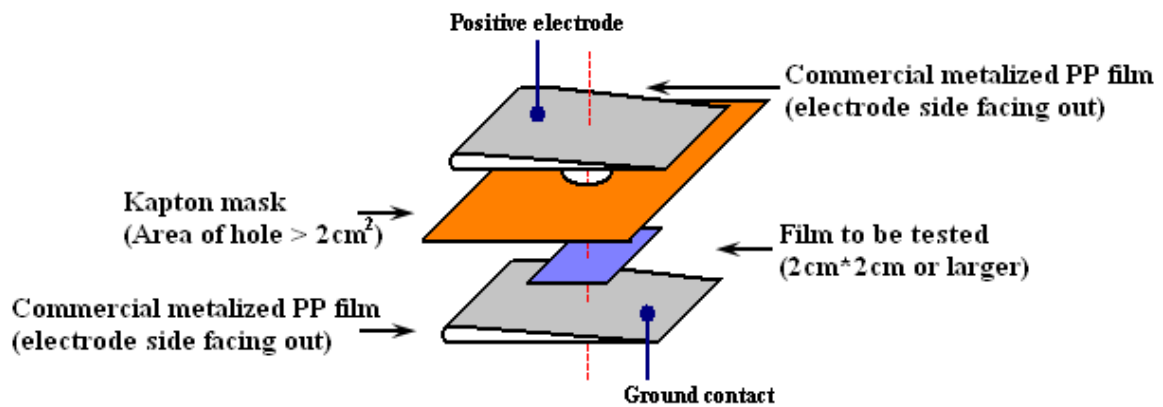


Figure 1-13: Setup diagram of electrostatic breakdown strength measurement.²⁵

The Kapton insulating mask separates the two electrodes, and its hole defines the spot where the breakdown strength is measured. While this method allows a measurement without prior damage to the film, it has the drawback that the electrode size cannot be too small. If the exposed areas of the electrode films are too small, they may not be in full contact with the measuring area due to the limited flexibility of the electrodes. Another reason to employ a relatively large electrode size is to minimize the overestimation of breakdown strength. Laihonon reported that the average breakdown strength of a film increased with the use of smaller electrodes.²⁶ Since large capacitor films are used in practical applications, it is of better interest to know the general breakdown strength that represents the whole film, not just the highest value of a single spot. For these reasons, the recently set standard measurement procedure by the Office of Naval Research (ONR) advises the use of electrode sizes that exceed 2 cm^2 .²⁵

1.5.3 Permittivity

Permittivity of a material describes the “ability of a material to polarize in response to an applied field,” which “reduces the total electric field inside the material.”²⁷ This parameter is important for capacitors, as materials with higher permittivity can store more charge under an applied voltage. In other words, they accumulate charge more efficiently than materials with low permittivity. In the characterization of a dielectric material, the permittivity of a material is expressed in terms of a dielectric constant, ϵ , which is the ratio of the permittivity of a material to the permittivity in vacuum (8.85×10^{-12} F/m). Dielectric constants of materials vary greatly. Polypropylene, a non-polar hydrocarbon, has a dielectric constant of 2.2, while polyvinylidene fluoride is reported to have a dielectric constant of 12.¹ Some other materials have higher dielectric constants, such as barium titanate, which has a dielectric constant of 1250²⁸. Materials with higher dielectric constants have a greater potential to store larger amounts of charges. In capacitor applications of these materials, however, both charging and discharging processes need to be considered. For instance, fluoropolymers can easily be poled under an applied electric field. However, there is a large charge loss during the discharging process as the inherently polar groups and large crystals do not return to the original, random state.²⁹ In the case of polypropylene, a non-polar polymer, its $-\text{CH}_3$ groups experience only induced polarization in the charging process. As a result, discharging eliminates the induced polarization which existed in the polymer matrix. Charge loss in the charging-discharging process is not favorable; however, high permittivity is an essential requirement for a high energy storage capacitor.

1.5.4 Polarization-depolarization Loop

The total charge accumulated on the surfaces of a capacitor per applied voltage is described using a polarization-depolarization loop. As the name indicates, this loop shows the changes in the surface charge during the charging and discharging processes. Representative polarization-depolarization loops of poly(vinylidene difluoride) (PVDF)² and polypropylene (PP) are shown in Figure 1-14. The U_e regions are the energy recovered, while domains under the curves are the energy loss. It is clear that PVDF stores much more charge than polypropylene even at a low field. The irreversibility of PVDF, indicated by the large hysteresis of energy loss, is not observed in the polypropylene polarization curve. As expected, the lost energy is released as heat. Higher energy losses liberate more heat, which may affect the stability of the capacitor film. For this reason, a film possessing a high thermal stability is favorable, and it is highly desirable to keep the energy loss to less than 1 % to maintain performance and film stability. In order to assess the energy storage capability of a capacitor material under practical application conditions, it is thus also important to evaluate the polarization-depolarization loop of a film.

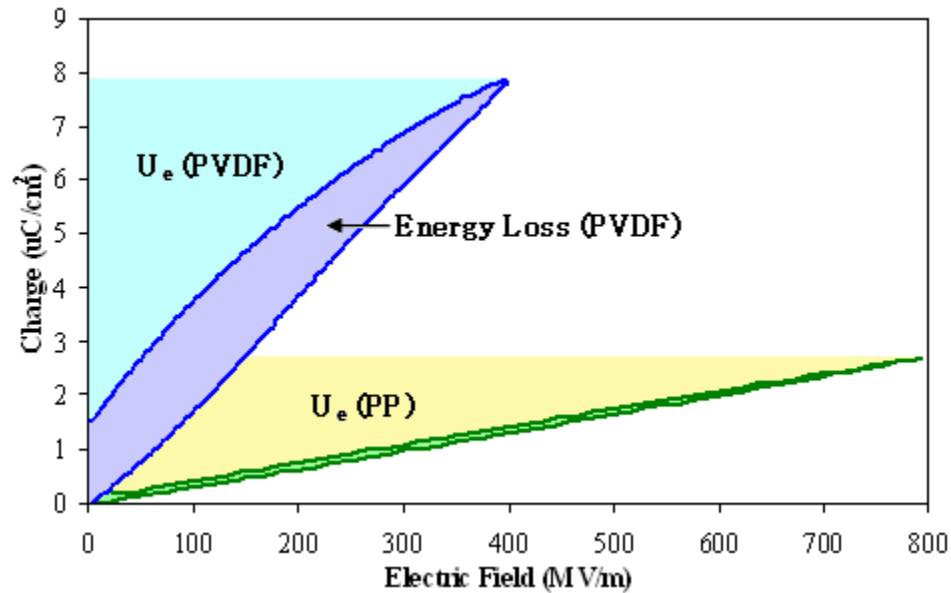


Figure 1-14: Representative polarization curves of PP and PVDF.² U_e is the energy recovered. Areas inside the loops are energy loss.

1.6 Polypropylene-based Capacitors

Among the polymers that are commonly used or studied for capacitor applications, polypropylene has a higher breakdown strength than others. Most reported breakdown strengths of polyethylene and poly(vinylidene fluoride-trifluoroethylene-chlorofluoroethylene) (p(VDF-TrFE-CFE) terpolymer derivatives are less than 600 MV/m ^{1, 29}, but the average breakdown strength of commercial biaxially oriented polypropylene films is approximately 700 MV/m .^{1, 23, 26, 29, 30} The low dielectric constant of polypropylene, 2.2, limits its overall energy density. Yet its low energy loss (Dissipation factor at 1 kHz, <0.02)¹ and high stability make it a commercially desirable and successful material in capacitor applications. In order to enhance the quality of a polypropylene film as a capacitor, it is essential that the breakdown strength and, more

importantly, the permittivity of the film are increased, possibly by functionalization with polar groups.

1.7 Conclusions

Polymer thin films are a favorable material for capacitors with a high power density storage requirement. In order to increase the energy stored per given volume of a capacitor, the polymer film needs to be processed into a thin film to maximize its surface area. Among the polymeric candidate materials, polypropylene is in a leading position as it has a statistically stable high breakdown strength and low energy loss.¹ It is thus beneficial to develop a polypropylene-based capacitor film.

Thermal processibility of isotactic polypropylene can be improved by the incorporation of long chain branches, which increases the melt strength of polypropylene. This improvement in melt strength allows isotactic polypropylene to embrace the whole spectrum of processing techniques available to prepare thin films.

One major drawback of polypropylene as a capacitor material is its low permittivity. It is essential to increase the dielectric constant of polypropylene for the development of a film capacitor with high energy density.

The main focus of this thesis is the improvement of a polypropylene-based capacitor film, and the objectives are to explore the synthesis of long chain branched polypropylene with better efficiency and to improve the dielectric properties of polypropylene and a similar polyolefin. The branching efficiency of T-reagents will be discussed in the first section of Chapter 2. In the following section, synthesis of new LCB polymers having polyethylene backbones and polypropylene side chains will be introduced. Effects of hydroxylation on the dielectric properties of non-polar polymers were investigated and will be discussed in Chapter 3. In this study,

favorable improvement in the dielectric constant was observed and desirable structures were identified. These findings will also be reported in Chapter 3.

References

1. Rabuffi, M.; Picci, G., Status quo and future prospects for metallized polypropylene energy storage capacitors. *Plasma Science, IEEE Transactions on* **2002**, 30, (5), 1939-1942.
2. Zhang, Z., PVDF Polarization Plot. In Data provided by courtesy of Dr. Zhang ed.; 2008.
3. Christen, T.; Carlen, M. W., Theory of Ragone plots. *Journal of Power Sources* **2000**, 91, (2), 210-216.
4. Nikkei Business Publications, I.
用途拡大の機運高まるチップ形積層フィルムコンデンサ.
http://techon.nikkeibp.co.jp/NEAD/focus/ped/ped_4.html (May 25),
5. Shizuki Tech Net Solution: Smoothing film capacitor for hybride vehicle inverter.
http://www.shizuki.co.jp/english/c_solution1.html (Feb 3, 2009),
6. Borchardt, J. K., Polymer composites bring a smile to dental fillings: Conference report. *Materials Today* **2005**, 8, (11), 19-19.
7. Smock, D. Boeing Dreamliner Drives Carbon Fiber Composites.
http://www.designnews.com/blog/Engineering_Materials/747-Boeing_Dreamliner_Drives_Carbon_Fiber_Composites.php (May 19),
8. Langston, J. A.; Colby, R. H.; Chung, T. C. M.; Shimizu, F.; Suzuki, T.; Aoki, M., Synthesis and Characterization of Long Chain Branched Isotactic Polypropylene via Metallocene Catalyst and T-Reagent. *Macromolecules* **2007**, 40, (8), 2712-2720.
9. Chung, T. C., Materials Science 441: Polymeric Materials. In 2006.
10. Y. S. Kim, C. I. C. S. Y. L. K. S. H., Melt rheological and thermodynamic properties of polyethylene homopolymers and poly(ethylene/alpha-olefin) copolymers with respect to molecular composition and structure. *Journal of Applied Polymer Science* **1996**, 59, (1), 125-137.
11. Imanishi, Y.; Naga, N., Recent developments in olefin polymerizations with transition metal catalysts. *Progress in Polymer Science* **2001**, 26, (8), 1147-1198.
12. Yan, D.; Wang, W. J.; Zhu, S., Effect of long chain branching on rheological properties of metallocene polyethylene. *Polymer* **1999**, 40, (7), 1737-1744.
13. Wen-jun Wang, D. Y. P. A. C. S. Z. A. E. H. B. G. S., Long chain branching in ethylene polymerization using constrained geometry metallocene catalyst. *Macromolecular Chemistry and Physics* **1998**, 199, (11), 2409-2416.
14. Esa Kokko, A. M. P. L. B. L. J. V. S., Influence of the catalyst and polymerization conditions on the long-chain branching of metallocene-catalyzed polyethenes. *Journal of Polymer Science Part A: Polymer Chemistry* **2000**, 38, (2), 376-388.
15. Xiaochuan Wang, C. T. G. L. R., Chemical modification of polypropylene with peroxide/pentaerythritol triacrylate by reactive extrusion. *Journal of Applied Polymer Science* **1996**, 61, (8), 1395-1404.
16. Weiqing Weng, E. J. M. A. H. D., Synthesis of vinyl-terminated isotactic poly(propylene). *Macromolecular Rapid Communications* **2000**, 21, (16), 1103-1107.
17. Graebbling, D., Synthesis of Branched Polypropylene by a Reactive Extrusion Process. *Macromolecules* **2002**, 35, (12), 4602-4610.
18. Beate Krause, D. V. L. H. D. A. H. M., Characterization of electron beam irradiated polypropylene: Influence of irradiation temperature on molecular and rheological properties. *Journal of Applied Polymer Science* **2006**, 100, (4), 2770-2780.
19. Auhl, D.; Stange, J.; Munstedt, H.; Krause, B.; Voigt, D.; Lederer, A.; Lappan, U.; Lunkwitz, K., Long-Chain Branched Polypropylenes by Electron Beam Irradiation and Their Rheological Properties. *Macromolecules* **2004**, 37, (25), 9465-9472.

20. Paavola, S.; Saarinen, T.; Lofgren, B.; Pitkanen, P., Propylene copolymerization with non-conjugated dienes and [alpha]-olefins using supported metallocene catalyst. *Polymer* **2004**, 45, (7), 2099-2110.
21. Roon, T. v. Capacitors Tutorial. <http://www.uoguelph.ca/~antoon/gadgets/caps/caps.html> (September 18),
22. November, P., Capacitor schematic with dielectric. In *Capacitor_schematic_with_dielectric.svg*, Ed. 2008.
23. Shihai Zhang, B. C., Xin Xhou, Bret Neese, Qiming Zhang *High Energy Density Polymer Dielectrics for Capacitor Applications*; Strategic Polymer Sciences, Inc., Penn State University: University Park, PA.
24. Fukuda, T., Technological progress in high-voltage XLPE power cables in Japan. I. *Electrical Insulation Magazine, IEEE* **1988**, 4, (5), 9-16.
25. Pan, M.-J., Electrostatic Breakdown Setup. In *Communication with Dr. Pan ed.*; 2008.
26. Laihonen, S. J.; Gafvert, U.; Schutte, T.; Gedde, U. W., DC breakdown strength of polypropylene films: area dependence and statistical behavior. *Dielectrics and Electrical Insulation, IEEE Transactions on* **2007**, 14, (2), 275-286.
27. Answers Corporation, Answers.com: Permittivity. In 2009.
28. Wikimedia Foundation, I., Relative Static Permittivity. In *Wikipedia*, 2009.
29. Zhang, Z.; Chung, T. C. M., Study of VDF/TrFE/CTFE Terpolymers for High Pulsed Capacitor with High Energy Density and Low Energy Loss. *Macromolecules* **2007**, 40, (4), 783-785.
30. Yutao, Z.; Ho Gyu, Y.; Suh, K. S., Electrical properties of silane crosslinked polyethylene in comparison with DCP crosslinked polyethylene. *Dielectrics and Electrical Insulation, IEEE Transactions on* **1999**, 6, (2), 164-168.

Chapter 2

Metallocene-mediated Synthesis of Long Chain Branched Polymer Containing Polyethylene and Polypropylene Using T-reagent

2.1 Introduction

Introducing long chain branches improves the melt strength of isotactic polypropylene and expands the choices of possible thermal processing techniques. As discussed in Chapter 1, various methods have been investigated for preparing long chain branched polypropylene (LCB PP). While successful in creating long chain branched structures, these synthetic routes have some drawbacks. Conversely, the one-pot synthesis of LCB PP polymers, developed in our laboratory, shows many promising results. This approach is free of degradation or reduction in the molecular weight, key problems in post-polymerization modifications. It is also unrestricted by crosslinking, a serious issue in the copolymerization of non-conjugated dienes at high concentrations.

The LCB PP polymers prepared by one-pot synthesis via butyl styrene or T-reagent were previously characterized by Langston et al.¹ Size exclusion chromatography (SEC) with triple detectors confirmed the presence of long chain branches, and rheological studies showed the strain hardening behavior of LCB PP. One of the areas in this preparation method that needed to be explored was the improvement of T-reagent efficiency, where only 15 to 25 % of BSt used in a typical reaction was consumed and where 50 % or less of the incorporated BSt is associated to long chain branches. Two approaches were taken to increase the T-reagent efficiency: increasing the ratio of long chain branches to styrene groups, and improving the T-reagent consumption through the synthesis of new polymers having polyethylene backbones and polypropylene side

chains. The breakdown strength of long chain branched and linear polypropylene will also be discussed in the latter part of this chapter.

2.2 Experiment

2.2.1 Materials and Instrumentation

The polymerization was carried out in a Parr Instrument 4500 stainless steel pressure reactor. All oxygen- and moisture-sensitive procedures were carried out in an argon-filled Vacuum Atmosphere dry box.

Toluene was refluxed over sodium metal and distilled under an argon atmosphere prior to use. Chemical grade ethylene and propylene gases, methylaluminoxane (MAO), and 1,1,2,2-tetrachloroethane-d₂ (99.6 % D) were used as received. P-(3-butenyl)styrene (BSt) was synthesized by a previously reported method.¹ Rac-dimethylsilanediylbis(2-methyl-4-phenylindenyl) zirconium dichloride was prepared by previous members of Chung's group at Penn State using previously reported methods.²

Commercial capacitor-grade isotactic polypropylene (EM 4342C2, EM iPP), obtained from ExxonMobil Chemical, and commercial branched high melt strength polypropylene (Daploy WB135HMS, HMS), obtained from Borealis, were used without further purifications.

All ¹H nuclear magnetic resonance (NMR) spectra were obtained using a Bruker AM 300 NMR at 110 °C, using 1,1,2,2-tetrachloroethane-d₂ as the solvent. Samples were purified by dissolving in boiling toluene and recrystallizing at room temperature. After washing repeatedly with a mixture of acetone and hexane, they were dried in a vacuum oven at 40 °C. NMR samples were prepared using the purified samples and deuterated tetrachloroethane. Typically, 64 scans were employed, although some samples required additional scans and the number of scans was increased as needed.

The melting temperatures of the polymers were measured using a TA Q100 differential scanning calorimeter (DSC). The melting transition was recorded while heating the samples from 40 to 180 °C at 20 °C/min, held isothermally for 3 min, cooled down to the initial temperature at 40 °C/min, then heated at 40 °C/min. T_m was determined from the second heating scan to eliminate effects from prior processing.

Thin films used in the breakdown strength measurements were all prepared by solution casting. A sample polymer was dissolved in boiling xylene and solution casted at 135 °C. Prepared films were dried in a vacuum oven at 130 °C for 6 hours.

Breakdown strength of the films were measured using a setup depicted in Chapter 1 (Figure 1-13). Electrode area was 2 cm². Applied voltage was increased at 500 V/s until the film failed.

2.2.2 Synthesis of Long Chain Branched Polypropylene via T-reagent

150 ml of dry toluene and 8 ml of MAO were added into a dry 450 ml Parr stainless steel autoclave equipped with a mechanical stirrer. 1 psi of hydrogen and 100 ml of liquid propylene monomer were added and the reactor was heated to 35 °C. P-(3-butenyl)styrene diluted in 3 ml toluene was introduced first while stirring the autoclave, followed by 1.0×10^{-6} moles of rac-Me₂Si[2-Me-4-Ph(Ind)]₂ZrCl₂ diluted in 1 ml of dry toluene. The reaction temperature was maintained at 38 °C. The reaction was terminated after 30 min using methanol. The product was washed with acidic methanol for one hour, rinsed with methanol, and dried under vacuum at room temperature.

2.2.3 Copolymerization of Ethylene and P-(3-butenyl)styrene

150 ml of dry toluene and 6 ml of MAO were added into a dry 450 ml Parr stainless steel autoclave equipped with a mechanical stirrer. 5 psi of hydrogen was added and the reactor was heated to 70 °C. Into a stirring autoclave, P-(3-butenyl)styrene diluted in 3 ml toluene was introduced first, followed by 1.5×10^{-6} moles of $\text{rac-Me}_2\text{Si}[2\text{-Me-4-Ph(Ind)}]_2\text{ZrCl}_2$ catalyst solution and 20 psi of ethylene monomer. The monomer was continuously fed while the reactor temperature was maintained at 70 °C. The reaction was terminated after 30 min using methanol. The product was washed with acidic methanol for one hour, rinsed with methanol, and dried under vacuum at room temperature.

2.2.4 Synthesis of LCB Polymers with PE Backbone and PP Side Chains

250 ml of dry toluene, 6 ml of MAO and 0.5 g of PE-BSt copolymer were added into a dry 450 ml Parr stainless steel autoclave. 1 psi of hydrogen was added, and then the reactor was heated to 80 °C. 1.0×10^{-6} moles of $\text{rac-Me}_2\text{Si}[2\text{-Me-4-Ph(Ind)}]_2\text{ZrCl}_2$ catalyst solution was introduced along with 100 psi of propylene monomer. The propylene monomer was continuously fed during the reaction. The reaction was stopped after 30 min using methanol. The product was washed with acidic methanol for one hour, rinsed with methanol, and dried under vacuum at room temperature.

2.3 Branching Efficiency in Metallocene-mediated Synthesis of LCB PP Using T-reagent

In a LCB PP synthesis via T-reagent, the incorporated BSt is associated either to the long chain branches or the pendant styrene group. It is interesting to note that ^1H NMR spectra indicate

that about 40 to 50 % of the incorporated BSt serve as branching points independent of reaction state (bulk or in solution), BSt concentration, and reaction time. Langston suggested that the similar branch/styrene ratio independent of reaction time may indicate that the incorporated BSt immediately undergoes chain transfer reaction, forms a branch, precipitates from solution and becomes inaccessible.¹ If this were the case, the branch/styrene ratio cannot be increased, as polypropylene would not completely dissolve in toluene under 110 °C, a temperature which is much higher than the reaction temperature. The original purpose of this study was to increase the BSt incorporation through a low-temperature reaction, which would also increase the absolute branch density in the polymer chain.

The synthesis of LCB PP via T-reagent produces three possible structures. The structures and ¹H NMR peak locations are illustrated in Figure 2-1. Typically structure 2, or the macromonomer, is not detected in a reaction. In fact, the 2g peak was not recognized in the spectra obtained in this study. Branches and styrene groups were distinguished using the aromatic proton peaks at 7.1, 7.2 and 7.4 ppm. Aromatic protons of branches produced only one peak at 7.1 ppm as they all had the same adjacent groups. Contrarily, the aromatic protons of pendant styrene had two peaks at 7.2 and 7.4 ppm from the -CH₂CH₂- and -CH=CH₂ nonsymmetrical phenyl ends.

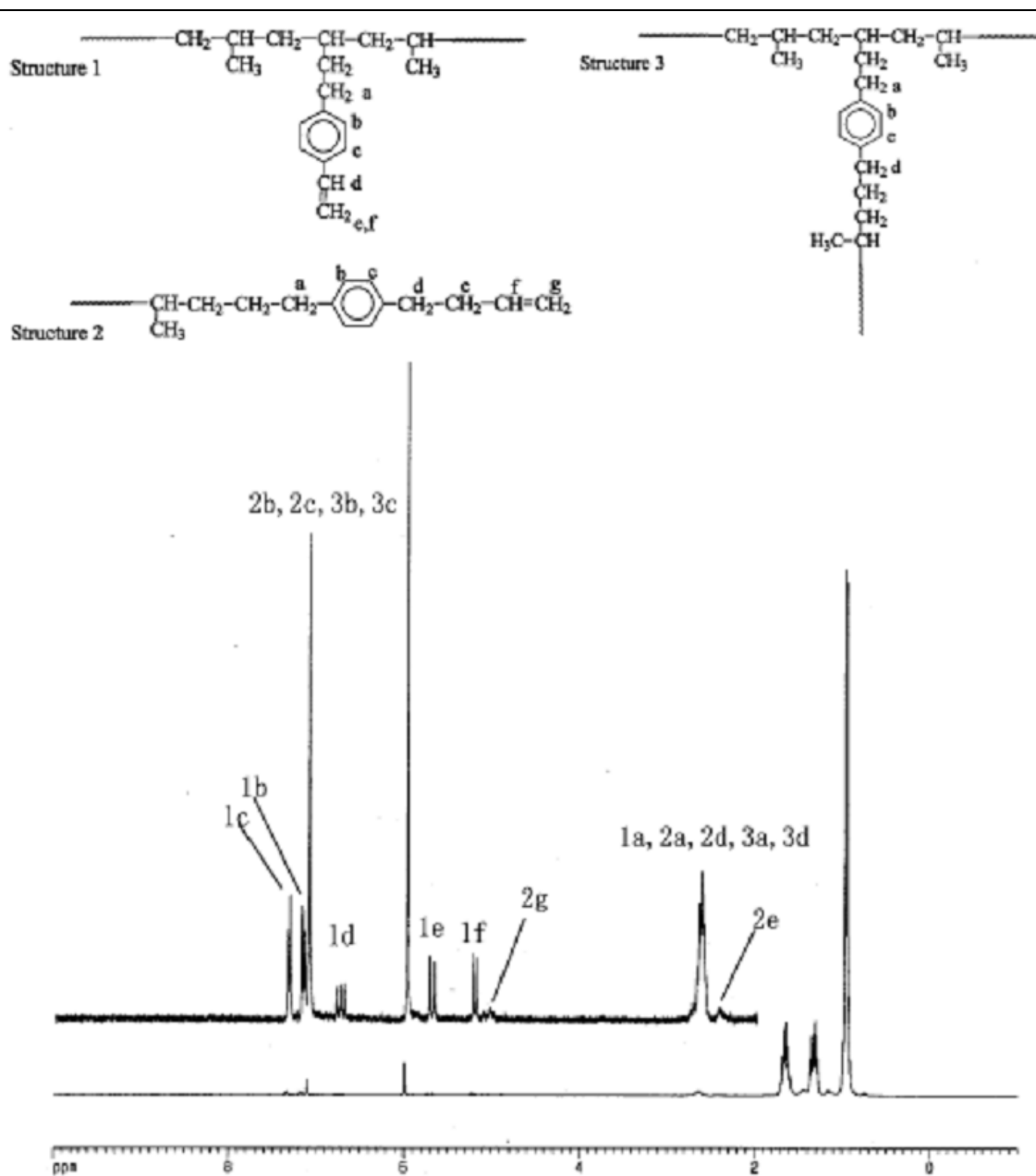


Figure 2-1: Representative ^1H NMR spectrum of LCB PP.¹

In this study, an increase in the long chain branch/styrene ratio was observed in low-temperature reactions. The ratio vs temperature plot is shown in Figure 2-2 with its corresponding data listed in Table 2-1. Figure 2-2 shows the temperature dependence of the branch/styrene ratio,

where aside from a few exceptional cases, the ratios were greater than 1 when the reactions were conducted below 37 °C. At temperatures exceeding 37 °C, the LCB/styrene ratio was less than 1.

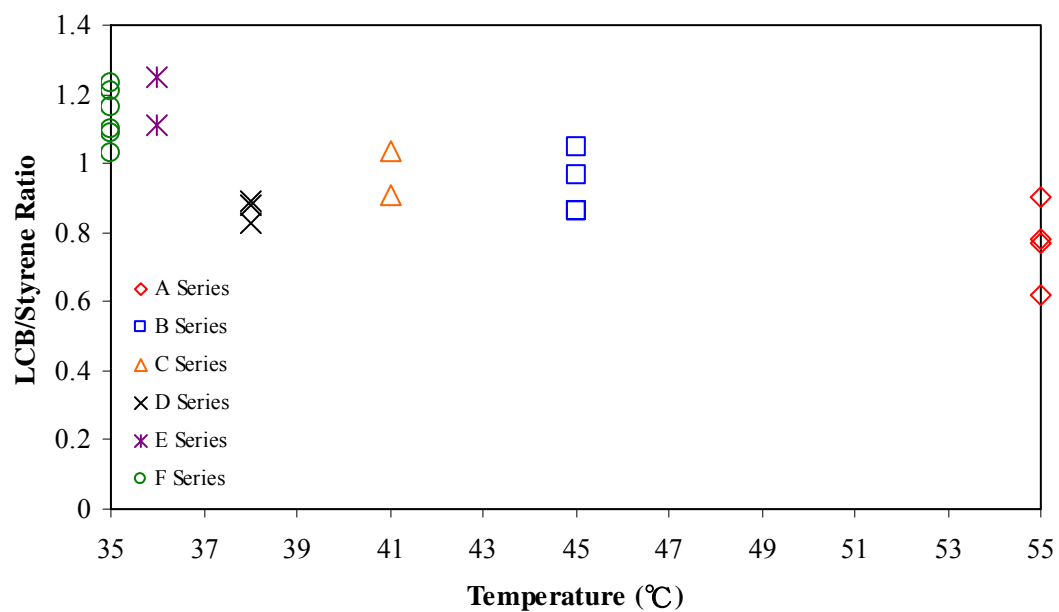


Figure 2-2: LCB/styrene ratio vs temperature plot. Details of each series are in Table 2-1.

Table 2-1: Summary of LCB PP polymers prepared by $\text{rac-Me}_2\text{Si}[2\text{-Me-4-Ph(Ind)}]_2\text{ZrCl}_2/\text{MAO}$ mediated bulk polymerizations.

	Reaction Conditions							Reaction Results			Polymer Structures					
	[BSt] ^a	Rxn Temp (°C)	Rxn Time (h)	Cat. ^b	H ₂ (psi)	Mon. ^c (ml)	Tol. ^d (ml)	Mon. Conv. ^e (%)	BSt Cons. ^f (%)	Cat. Act. ^g	BST Incorpor. ^h (mol %)	LCB (mol %)	St. Group ⁱ (mol %)	Bran. Den. ^j	Mv. ^k	LCB/St. Ratio ^l
A-1	0.10	55	0.33	0.5	1	100	50	21	26	41	0.12	0.05	0.07	1.74	273.4	0.77
A-2	0.20	55	0.33	0.5	1	100	50	16	14	36	0.17	0.08	0.09	2.68	173.3	0.90
A-3	0.26	55	0.33	0.5	1	100	50	23	19	51	0.22	0.08	0.13	2.66	106.1	0.62
A-4	0.40	55	0.5	0.5	1	100	50	18	16	23	0.35	0.14	0.19	4.79	84.2	0.78
B-1	0.025	45	0.13	1.7	1	100	300	27	42	61	0.04	0.02	0.02	0.62	121.7	0.86
B-2	0.05	45	0.13	1.7	5	100	300	16	19	37	0.06	0.03	0.03	0.96	100.2	0.97
B-3	0.1	45	0.13	1.7	5	100	300	37	17	84	0.05	0.02	0.02	0.75	85.2	1.05
B-4	0.1	45	0.13	1.7	10	100	300	37	25	84	0.07	0.03	0.04	1.05	68.5	0.86
C-1	0.025	41	0.08	0.6	1	100	70	14	14	86	0.04	0.02	0.02	0.74	463.4	1.04
C-2	0.1	41	0.08	0.6	1	100	70	21	21	128	0.09	0.04	0.05	1.36	307.5	0.91
D-1	0.2	38	0.5	1	1	50	150	68	14	35	0.04	0.02	0.02	0.64	-	0.83
D-2	0.4	38	0.5	1	1	50	150	48	8	25	0.07	0.03	0.04	1.06	-	0.89
D-3	0.8	38	0.5	1	1	100	150	75	34	77	0.19	0.09	0.10	2.94	-	0.88
E-1	0.2	36	1	1	1	50	150	34	38	21	0.10	0.05	0.05	1.68	195.0	1.11
E-2	0.3	36	1	1	1	50	150	62	59	38	0.12	0.07	0.05	2.20	425.8	1.25
F-1	0.2	35	0.42	1	1	150	75	27	26	10	0.19	0.10	0.09	3.46	184.4	1.16
F-2	0.2	35	0.75	1	1	150	75	41	27	31	0.13	0.07	0.06	2.32	232.0	1.21
F-3	0.2	35	2	1	1	150	75	40	30	15	0.15	0.08	0.07	2.63	369.6	1.10
F-4	0.3	35	0.66	1	1	150	75	41	24	47	0.18	0.10	0.08	3.34	270.9	1.23
F-5	0.3	35	0.75	1	1	150	75	29	21	22	0.22	0.11	0.11	3.79	252.5	1.09
F-6	0.3	35	1.25	1.5	1	150	200	41	15	21	0.11	0.06	0.06	1.91	127.5	1.03

a. [BSt]/[Propylene] (mol %)

b. Catalyst: (μmol)

c. Monomer: liquid propylene (ml)

d. Toluene (ml)

e. Monomer conversion: (w/w %)

f. BSt consumption: (w/w %)

g. Catalyst Activity: (kg of PP/(mmol of Zr-h))

h. BSt incorporation (mol %)

i. Styrene group: (mol %)

j. Branch density: (branch points/10,000 carbons)

k. Mv: viscosity molecular weight (kg/mol)

l. LCB/styrene ratio: (LCB mol %/styrene group mol %)

Typically, propylene is polymerized around 40 to 50 °C to maintain a high catalyst reactivity. Comparison of the A to D series, summarized in Table **2-1**, showed that the branch/styrene ratio was not affected by the BSt concentration, reaction time, hydrogen pressure, monomer/solvent ratio, monomer conversion, nor BSt consumption. Despite the intermediate reaction time and greatly varied BSt concentration, the branch/styrene ratios obtained in the D series were very similar between 0.83 and 0.89. These ratios observed in high temperature reactions were in good agreement with the trend reported by Langston, who synthesized LCB PP polymers in solution at 55 °C.¹ The fact that these variables have no effect on the branch/styrene ratio confirms the interpretation given by Langston, where a growing polymer chain quickly chain transfers to a pending styrene group, precipitates, and the incorporated styrene group becomes inaccessible for further chain transfer.¹

In the low-temperature reactions (below 37 °C) the branch/styrene ratios suddenly increased. The experimental results of the E and F series are in Table **2-1**. Reaction times were increased to compensate for the expected reduction in the catalyst reactivity due to the lower reaction temperature. Similar to the high temperature reactions, no clear general dependency was observed in the branch/styrene ratio; however, it is apparent that the lower reaction temperatures resulted in higher branch/styrene ratios. Nevertheless, there are some clues which may help to explain the limitation of a further increase in the ratios. The monomer and BSt conversions of F-2 to F-4 samples were similar, despite the large difference in reaction times. The estimated amount of polymer from 150 ml liquid propylene with 40 % conversion is about 30 g. Considering that 75 ml of solvent was used, the ratios of F-2 to F-4 reactions probably were already at their maxima as no further reaction was able to occur. This raises a question: would it be possible to increase the ratios further if these needs are fulfilled?

E-1 and E-2 both had a sufficient amount of solvent, monomer and BSt to carry out the reaction further if needed. Comparing these samples, the branch/styrene ratio did not increase

much despite their intermediate reaction time and reaction conditions, which allowed for relatively high BSt consumptions. This may suggest that the rates of branch formation in the low-temperature reactions were independent of reaction conditions due to the branch/styrene ratios that were obtained.

A possible explanation for the increase in the LCB/styrene ratio with a reduction in reaction temperature could arise from the stability of the dormant catalyst site, resulting from the chain transfer of the growing polymer chains to the pendant styrene groups. As previously depicted in Figure 1-10, the formation of long chain branches involves two steps: chain transfer of growing polymer chains to the styrene group (Figure 1-10, structure (V)) and chain transfer to hydrogen, which results in the reactivation of the catalyst. Perhaps the product of the first step is a stable species, which makes this step kinetically favorable for the termination of the growing polymer chains rather than termination by β -hydride elimination. Generally, styrene is a reactive group which can react at low temperature. The increase in the LCB/styrene ratios in the reactions at low temperatures, below 37 °C, may suggest that the reduction in the reaction temperature favors the formation of a stable structure, where the styrene group is chain transferred by the growing polymer chains, which lead to the formation of more long chain branches relative to the styrene group.

2.4 New LCB Polymers Having PE Backbone and PP Side Chains

One drawback of the one-pot synthesis of LCB PP via T-reagent is the T-reagent inefficiency. In a typical reaction at high temperature with 30 to 40 % propylene conversion, 15-25 % of BSt is consumed and of the incorporated BSt, 40 to 50% is associated to long chain branches. As suggested by Langston and shown in the previous section, this restriction is due to the ease with which polypropylene precipitates and its inaccessibility to the incorporated pendant

styrene.¹ One way to keep the BSt incorporated polymer chain completely dissolved in solution is to create the polymer backbone using polyethylene. Polyethylene has a lower melting temperature than polypropylene and it also dissolves in toluene at a lower temperature. The key in this approach is to keep the polymer backbone in solution as long as possible. It is, therefore, important either to consume all the BSt during the polyethylene-BSt copolymerization or to wash out the unreacted BSt after the copolymerization.

In this study, a two-step process was adopted to check the BSt consumption during the polyethylene-BSt copolymerization. This allowed for a better understanding of the polyethylene-BSt backbone, and allowed us to observe changes during the copolymerization of PE-BSt and propylene.

2.4.1 PE-BSt Copolymers Having LCB Structures

The presence of hydrogen plays an important role in a propylene-BSt copolymerization as previously shown by Dong and Langston. The amount of hydrogen present influences the catalyst reactivity, molecular weight, and long chain branch concentration.^{1, 3} Similarly, the presence of hydrogen affects the copolymerization of ethylene and BSt. The role of hydrogen in a PE-BSt copolymerization can be interpreted from the experimental results in Table 2-2. Except for PE-BST 1, ethylene-BSt copolymerizations in the absence of hydrogen contained insoluble portions which were visually observable in a 1 % w/v polymer solution. In the reactions with different pressures of hydrogen, 1 to 10 psi, the 1 % w/v polymer solution was visually transparent. As previously shown by Dong using ethylene-p-methylstyrene copolymerization, the incorporated p-methylstyrene could undergo two possible reactions: reaction with ethylene to form polyethylene-p-methylstyrene copolymer or reaction with hydrogen to create p-methylstyrene terminated polyethylene.⁴ A similar case also applied here, however there were

two major differences. First, the allyl end of BSt was more reactive than styrene end when using the $\text{rac-Me}_2\text{Si}[2\text{-Me-4-Ph(Ind)}]_2\text{ZrCl}_2$ catalyst. Second, the product structures were more complicated in the ethylene-BSt copolymerization than in the ethylene-p-methylstyrene copolymerization. The styrene groups of the incorporated BSt served as branch points, and branched and pseudo-crosslinked structures were formed. Illustrations of the two possible product structures are shown in Figure 2-3.

Table 2-2: Summary of PE-BSt copolymers by $\text{rac-Me}_2\text{Si}[2\text{-Me-4-Ph(Ind)}]_2\text{ZrCl}_2/\text{MAO}$ mediated in solution polymerizations.

	Reaction Conditions			Reaction Results		Polymer Structures				
	BSt (g)	Hydrogen (psi)	Reaction Time (h)	Product (g)	Catalyst Reactivity (kg/mmol-h)	BSt Incorporation (mol %)	Styrene Group (mol %)	Branch Density (mol %)	BSt Consumption (%)	Completely Soluble?
PE-BST 1	0.4	0	0.5	1.49	2.0	1.49	0.92	0.56	29	Yes
PE-BST 2	0.4	0	0.5	4.76	6.3	0.71	0.51	0.20	19	No
PE-BST 3	0.4	0	1.5	4.43	2.0	1.06	0.62	0.43	63	No
PE-BST 4	0.4	5	0.5	2.89	3.8	1.54	0.53	1.01	58	Yes
PE-BST 5	0.4	5	1.0	4.25	2.8	1.38	0.46	0.85	78	Yes
PE-BST 6	0.4	10	1.0	1.76	1.2	1.61	1.13	0.47	40	Yes
PE-BST 7	0.1	5	1.0	2.58	1.7	0.76	0.52	0.24	100	Yes
PE-BST 8	0.1	1	1.0	2.69	1.8	0.69	0.45	0.19	100	Yes
PE-BST 9	0.1	5	0.5	2.56	3.4	0.88	0.60	0.28	100	Yes
PE-BST 10	0.1	1	0.5	1.90	2.5	1.01	0.67	0.34	100	Yes

* Reaction temperature: 70 °C

* Solvent: 150 ml

* Catalyst concentration: 1.5 μmol

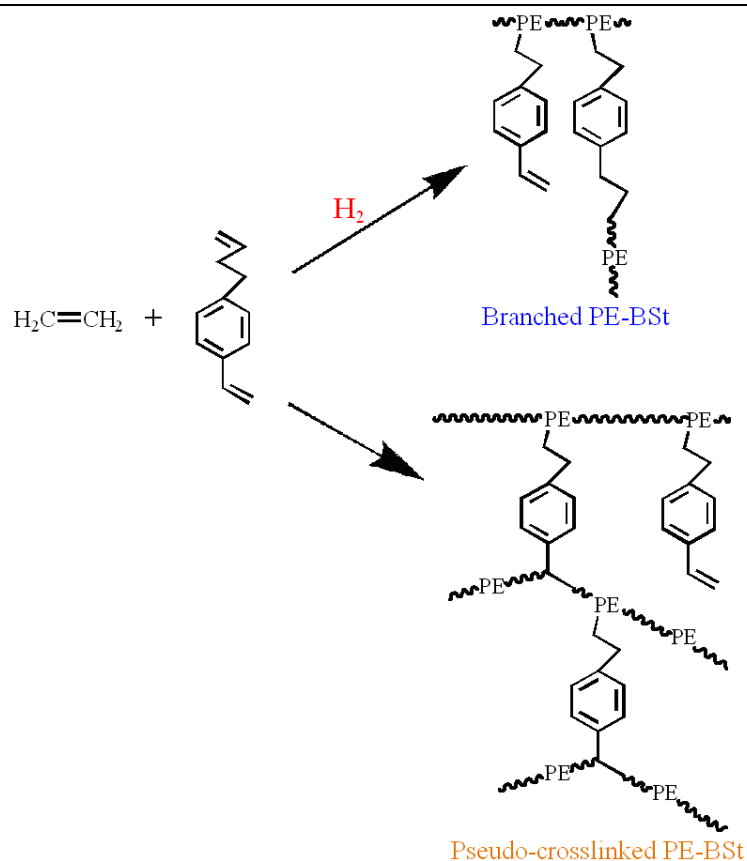


Figure 2-3: Schematic of the two possible structures produced in a copolymerization of ethylene and butyl styrene. Reaction with the presence of hydrogen produces branched PE-BSt. Reaction without hydrogen produces pseudo-crosslinked PE-BSt.

The presence of polyethylene branches and crosslinked structures were also observed in the ^1H NMR results. In a ^1H NMR spectrum of long chain branched polyethylene or polypropylene prepared via BSt, there were three peaks between 7.0 and 7.4 ppm. These peaks were proton peaks of the phenyl group in BSt. The left two peaks around 7.2 and 7.4 ppm were protons of a phenyl group with an allyl group adjacent to it. The peak at 7.1 ppm was from protons of a symmetrical phenyl group with saturated carbons as its nearest neighbors. In the spectra of reactions with and without hydrogen, all three peaks were present. If the peak at 7.1 was solely from long chain branches, the product should be completely soluble. Conversely, if the incorporated BSts were serving as crosslink points and the created pseudo-crosslinked network

was big, then a portion of the product would be insoluble. In ethylene-BSt copolymerizations, PE-BSt 2 and 3 contained insoluble portions while others, except PE-BST 1, were completely soluble. The major difference between those three samples and the rest was the presence of hydrogen in the reaction. The samples prepared with the presence of hydrogen, PE-BSt 4-10, were expected to contain some long chain branches based on their solubility and ethylene-p-methylstyrene studies by Dong.⁴ PE-BSt 2 and 3 also had a peak at 7.1 ppm yet contained insoluble portions. This must be an indication that the 7.1 ppm peak in PE-BSt 2 and 3 was of the protons of BSt whose phenyl groups were incorporated into neighboring polyethylene chains and formed a crosslink network.

2.4.2 LCB Polymers with PE Backbone and PP Side Chains (PE-BSt-PP)

The ethylene-butylstyrene copolymerization was investigated in the previous section, and high consumption of BSt (100 %) was attained in the reactions where 0.1 g of BSt was employed. The resulting PE-BSt copolymer, using styrene units, was further applied to prepare LCB polymer having PE backbone and PP side chains.

PE-BSt 5 was used in this study. It had BSt incorporation of 1.38 mol %, of which 0.46 mol % was styrene group and 0.85 mol % was branches. ¹H NMR spectra of representative PE-BSt and PE-BSt-PP are shown in Figure 2-4. Results of several PE-BSt-PP copolymerizations are summarized in Table 2-3. The sharp intense peaks at 7.2 and 7.4 ppm, which were present prior to the PE-BSt-PP copolymerization, diminished with the complete consumption of the styrene double bonds, and the single peak at 7.1 ppm increased proportionally. This was due to the formation of polypropylene long chain branches. The polyethylene peak at 1.6 ppm also diminished, and the polypropylene peaks at 0.95, 1.3, and 1.6 ppm appeared, indicating the predominance of polypropylene. Styrene groups were not completely consumed when they were

present in high concentration, as represented in PE-BSt-PP 1. There are two explanations of the limitation. First, the catalyst used, $\text{rac-Me}_2\text{Si}[2\text{-Me-4-Ph(Ind)}]_2\text{ZrCl}_2$, favors the incorporation of the allyl end of BSt. During the PE-BSt and propylene copolymerizations, the reaction temperature was maintained at 80 °C to keep PE-BSt completely in solution, allowing for better access to the styrene groups. The high reaction temperature, however, also increased the catalyst reactivity, which speeded up the propylene homopolymerization. As a result, the increased amount of product polymer promoted the precipitation of polymers from the reaction solution. In addition, the high reaction temperature induced the termination of propylene polymerization via beta-hydride elimination more than by chain transfer to the styrene groups. The ^1H NMR spectra of PE-BSt-PP showed peaks around 5.1 and 4.8 ppm, which were from the vinyl peaks of polypropylene chain ends.⁵⁻⁷ The intensity ratio of branches to chain end vinyl peaks indicated that the concentration of the terminal vinyl groups in the samples was higher than that of branches. Synthesis of PE-BSt copolymer with lower molecular weight is highly desirable in future runs to dissolve and copolymerize with propylene at lower temperature, such as 70 or 75 °C, which will reduce beta-hydride elimination.

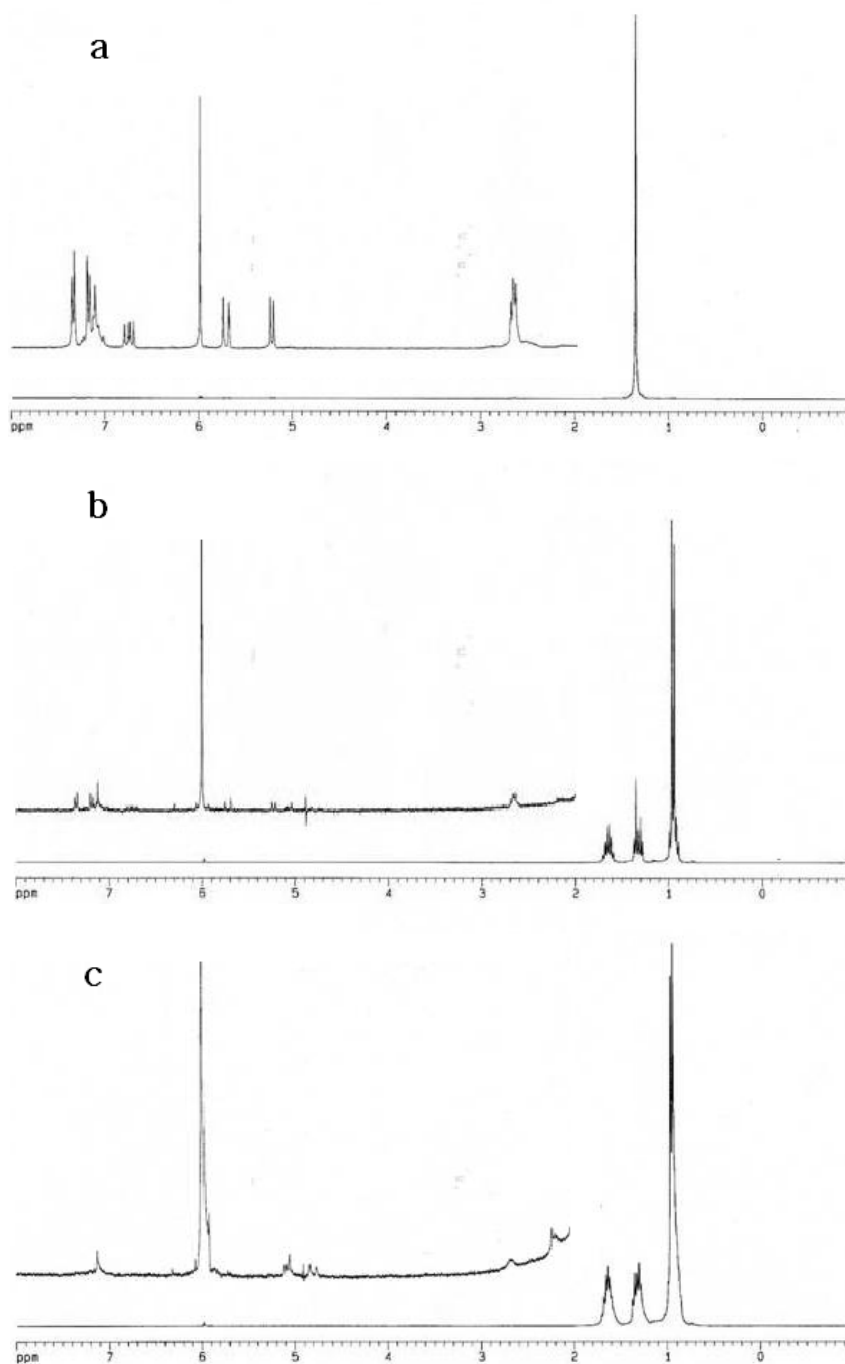


Figure 2-4: ^1H NMR spectra of PE-BSt and PE-BSt-PP with different pending styrene consumptions. (a) PE-BSt, (b) PE-BSt-PP 1 with 77 %, and (c) PE-BSt-PP 2 with 100 % consumption.

Table 2-3: Summary of PE-BSt and propylene copolymerizations.

	PE-BSt 5 Used (g)	Catalyst (μmol)	% Styrene Consumed	LCB Brances (mol %)	PP T_m ($^{\circ}\text{C}$)	PE/PP wt %
PE-BSt-PP 1	1.0	1.0	77	0.03	163	4.1
PE-BSt-PP 2	0.5	2.5	100	0.02	163	1.1
PE-BSt-PP 3	0.3	2.5	100	0.01	161	0.7
PE-BSt-PP 4	0.3	2.0	100	0.01	164	0.6

The branched structures with PE backbone and PP side chains were further analyzed using DSC. PE-BSt 2 exhibited the polyethylene melting peak around 130 $^{\circ}\text{C}$. The magnitude of the polyethylene peaks was greatly reduced even in the incomplete reaction, PE-BSt-PP 1, and it diminished with the complete consumption of the styrene groups in PE-BSt-PP 2, 3, and 4 (Figure 2-5). With the complete consumption, the T_m of polypropylene in PE-BSt-PP 2 and 3 shifted to lower temperatures. The T_m of polypropylene in PE-BSt-PP 1 remained high in spite of its high content of polyethylene, due to the polypropylene homopolymer which was not grafted onto a polyethylene backbone. The T_m of polypropylene in PE-BSt-PP 4 was also at a high temperature, due to the low concentration of polyethylene in the branched structure. The polyethylene backbone and branches reduced the melting temperatures by a few degrees, indicating the predominance of polypropylene and retainment of the desirable properties of polypropylene.

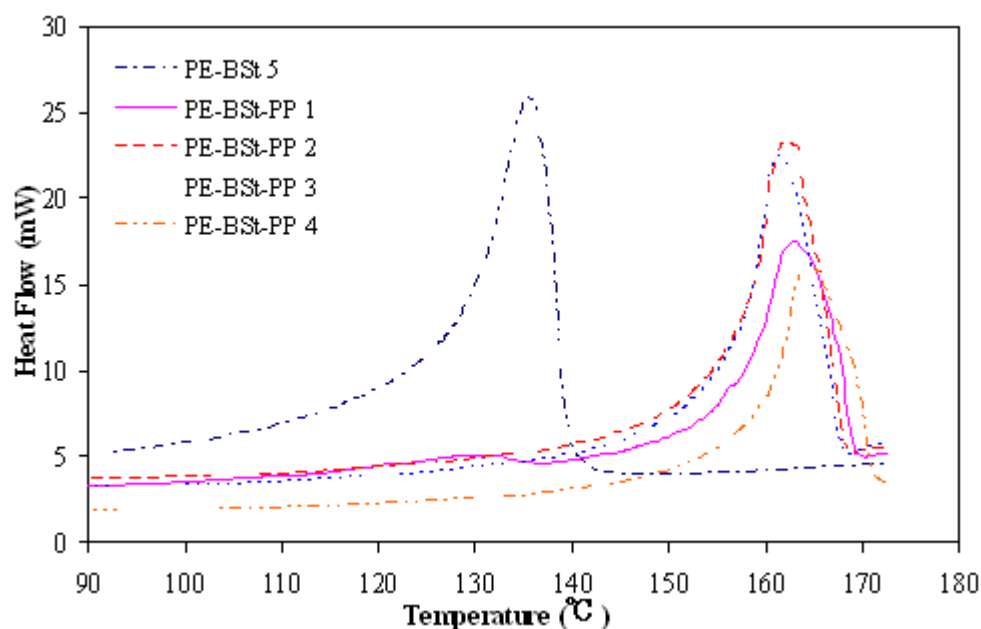


Figure 2-5: Melting temperatures (T_m) of PE-BSt and PE-BSt-PP samples.

2.5 Breakdown Strength of Linear and Branched Polymers

The breakdown strength of linear and branched polypropylene films was statistically characterized using Weibull analysis. Weibull analysis involves two parameters, alpha and beta, where when ten or more samples are tested, alpha is the characteristic breakdown strength when 63.2 % of the tested samples failed, and beta is a shape parameter that describes the distribution of breakdown strengths.⁸ The narrower the distribution is, the higher the beta value.

Three long chain branched polypropylenes (LCB) with different branch densities prepared in the lab, commercial branched high melt strength polypropylene (HMS), and commercial capacitor grade linear polypropylene (EM) were compared. General properties and Weibull values are summarized in Table 2-4. Weibull plots of the breakdown strengths are shown in Figure 2-6.

Table 2-4: Breakdown strength analysis of different linear and branched polypropylene using Weibull analysis.

	Branch/10,000 carbons	Alpha	Beta
EM	-	417	2
HMS	-	344	13
LCB 1	3.9	372	9
LCB 2	7.0	388	16
LCB 3	11	355	9

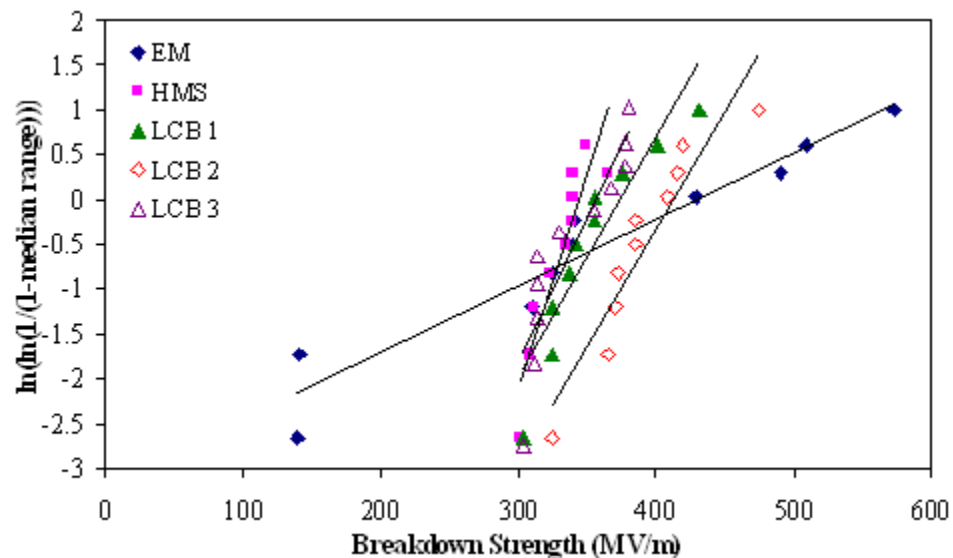


Figure 2-6: Weibull plots of EM, HMS and LCB breakdown strengths measured at room temperature.

The alpha values of EM, HMS and LCB had similar ranges, between 344 and 417 MV/m, with EM having the highest value. There was a greater, notable difference in the beta value. The high-end breakdown strengths of EM observed were above 500 MV/m. Despite these high breakdown strengths, its beta was low at 2, due to its defects. In practical applications, a high Weibull breakdown strength (alpha) and a narrow distribution (beta) are required for a stable, reliable capacitor film. In this respect, the presence of branches improved both alpha and beta when the films were all prepared in a similar manner by solution casting. It is interesting to note

that the improved alpha and beta in LCB 2 declined with a further increase in the branch density. These changes can likely be attributed to the reduction in the molecular weight of LCB 3, which made the LCB 3 film less stable during the thermal treatments employed in the film preparation. In the LCB PP synthesis via T-reagent, the employment of higher concentration of BSt reduces the catalyst reactivity and molecular weight of product polymers. This probably is a good assumption, as three times higher concentration of BSt was used in the synthesis of LCB 3 than LCB 1.

2.6 Conclusions

In an attempt to improve the T-reagent efficiency, a low reaction temperature system was studied and a long chain branched polymer containing polyethylene backbone and polypropylene branches was synthesized.

In a typical reaction at high temperature, there is more pendant styrene than long chain branches. Under low reaction temperature conditions, below 37 °C, the ratio of LCB/styrene ratio increased to above 1, indicating the presence of more branches than pendant styrene groups. A possible explanation of the increase in the LCB/styrene ratio with a reduction in reaction temperature may be the stability of the dormant catalyst site, resulting from the chain transfer of growing polymer chains to the pendant styrene groups. Perhaps the structure formed is a stable species, which makes the chain transfer of growing polymer chains to the pendant styrene groups kinetically more favorable than the termination of growing polymer chains by β -hydride elimination.

New LCB polymers having PE backbone and PP side chains were then synthesized to utilize all the T-reagent. Copolymerization of PE-BSt successfully consumed all the BSt used and produced LCB PE when reacted in the presence of hydrogen. The copolymerization of PE-BSt

and propylene consumed all the pendant styrene groups at low concentration. Despite the incomplete consumption of styrene groups when high concentrations of styrene groups were used, copolymerization of PE-BSt and propylene created a branched structure having a PE backbone with PP side chains.

The breakdown strength analysis of commercial linear and branched polypropylene, and LCB PP prepared via the T-reagent exhibited a reduction in fatal defects in LCB PP and increase in the overall stability of the film. Film preparation techniques must be improved to achieve higher breakdown strength; however, it appears that the presence of long chain branches increases both Weibull alpha and beta values.

References

1. Langston, J. A.; Colby, R. H.; Chung, T. C. M.; Shimizu, F.; Suzuki, T.; Aoki, M., Synthesis and Characterization of Long Chain Branched Isotactic Polypropylene via Metallocene Catalyst and T-Reagent. *Macromolecules* **2007**, 40, (8), 2712-2720.
2. Spaleck, W.; Kueber, F.; Winter, A.; Rohrmann, J.; Bachmann, B.; Antberg, M.; Dolle, V.; Paulus, E. F., The Influence of Aromatic Substituents on the Polymerization Behavior of Bridged Zirconocene Catalysts. *Organometallics* **1994**, 13, (3), 954-963.
3. Chung, T. C.; Dong, J. Y., A Novel Consecutive Chain Transfer Reaction to p-Methylstyrene and Hydrogen during Metallocene-Mediated Olefin Polymerization. *Journal of the American Chemical Society* **2001**, 123, (21), 4871-4876.
4. Dong, J. Y.; Chung, T. C., Synthesis of Polyethylene Containing a Terminal p-Methylstyrene Group: Metallocene-Mediated Ethylene Polymerization with a Consecutive Chain Transfer Reaction to p-Methylstyrene and Hydrogen. *Macromolecules* **2002**, 35, (5), 1622-1631.
5. Weiqing Weng, E. J. M. A. H. D., Synthesis of vinyl-terminated isotactic poly(propylene). *Macromolecular Rapid Communications* **2000**, 21, (16), 1103-1107.
6. Hisayuki Nakatani, S. S. T. T. M. T., Effect of unsaturated chain end-group on thermal oxidative behavior of polypropylene. *Polymer International* **2007**, 56, (9), 1147-1151.
7. Carvill, A.; Tritto, I.; Locatelli, P.; Sacchi, M. C., Polymer Microstructure as a Probe into Hydrogen Activation Effect in ansa-Zirconocene/Methylaluminoxane Catalyzed Propene Polymerizations. *Macromolecules* **1997**, 30, (23), 7056-7062.
8. Dorner, W. W. Using Microsoft Excel for Weibull Analysis.
http://www.qualitydigest.com/jan99/html/body_weibull.html

Chapter 3

Functional Polyolefin-based Capacitors for Energy Storage

3.1 Introduction

Polypropylene is one of the leading materials in film capacitor applications, as discussed in Chapter 1, due to its high breakdown strength, low energy loss and reliability. The low dielectric constant of polypropylene, $\epsilon=2.5$, limits its ability to accumulate a large amount of charge, resulting in a low energy density (1 to 1.2 J/cm³) for a polypropylene-based capacitor, relative to its high breakdown strength.¹ It is, therefore, necessary to introduce polar groups to increase the polarization within the dielectric matrix.

Among various polar groups, fluorine is by far the most popular group. In terms of functionalization chemistry, however, it is not readily available. In elementary stages, fluorine is highly reactive and exothermic.² Thus, fluorination of a polymer is conducted at room temperature. While this is convenient, direct fluorination at room temperature has a major drawback in that only the surfaces are modified.²⁻⁴ In addition, fluorine non-selectively replaces the hydrogen atoms of the modified polymer.^{3, 4} Conversely, a hydroxyl group is more suitable for the functionalization of hydrocarbon polymers. The hydroxyl (OH) group is polar and possesses an estimated dipole moment of approximately 1.6 D, which is similar to the dipole moment of poly(vinylidene fluoride) (PVDF), 2.1⁵. In addition, a simple comparative estimation of the dielectric constant of a hydroxylated polymer, relative to the unmodified polymer, suggests a potential approach. It is known that a random distribution of trifluoroethylene (TrFE) in a P(VDF-TrFE) copolymer helps to direct the VDF polar groups to all trans or polar conformation.⁶ The dielectric constant of the totally poled VDF groups in a P(VDF-TrFE) copolymer is about

80^7 , which is more than 6 times higher than the typical dielectric constant of PVDF (12).¹ The hydroxylated polymers studied here have one O-H bond, half the number of C-F bonds in PVDF, which halves the estimated dielectric constant, $80 / 2 = 40$. The estimated value is further reduced as the hydroxyl bond has a lower dipole moment than that PVDF. With this in consideration, the dielectric constant of a hydroxylated polymer is expected to be about $40 * 1.6 / 2.1 = 30$. This simple estimated value is not as high as that of fluoro group terpolymers. Nevertheless, this would intensify the dielectric constant of polypropylene by roughly 12 times, a significant improvement in the dielectric constant. Furthermore, hydroxylation chemistry was previously studied in our group⁸⁻¹⁰, and the functionalization effect on the dielectric response could be investigated in a relatively short time. With these advantages, the hydroxyl functionality was chosen as the polar group to increase the dielectric constant of a polypropylene-based capacitor.

The hydroxylation chemistry studied in our group involves a hydroboration-oxidation process. In this reaction, olefins are first reacted with 9-borabicyclononane (9-BBN), then oxidized in the subsequent reaction. If a double bond is present, it is possible to hydroxylate the polymer main chain or a branch end. In this hydroxyl dielectrics study, two types of structures were examined. In the first section, polypropylene-butyl-OH (PP-OH) was studied. This structure has the hydroxyl groups at the end of incorporated butyl branches, which gives OH groups extra mobility. Further incorporation of comonomer was not feasible due to the rapid reduction in the catalyst reactivity. Thus, an alternative study model was adopted. In the latter section, hydroxylated polybutadiene (PB-OH), poly(vinyl alcohol-co-ethylene) (PVA-co-PE), and polyvinyl alcohol (PVA), all with higher hydroxyl content than PP-OH, were investigated. These samples provide information on the dielectric effects from hydroxyl groups that are highly concentrated and less mobile, since the -OH groups are attached to the polymer backbone. A wide range of hydroxyl group contents was covered, and their hystereses in the heating-cooling scans in the dielectric constant measurements were also examined.

3.2 Experiment

3.2.1 Materials and Instrumentation

Propylene and hexenyl-9-BBN copolymerizations were carried out in a Parr Instrument 4500 stainless steel pressure reactor. All oxygen and moisture sensitive procedures were carried out in an argon-filled Vacuum Atmosphere dry box. Hydroboration and oxidation of polybutadiene were carried out in a 2 L three-neck, round-bottom flask while maintaining positive internal pressure.

Toluene was refluxed over sodium and distilled under an argon atmosphere prior to use. Chemical-grade propylene, methylaluminoxane (MAO), 0.5 M 9-BBN in tetrahydrofuran, and 1,1,2,2-tetrachloroethane- d_2 (99.6 % D) were used as received. Rac-dimethylsilanediylbis(2-methyl-4-phenylindenyl) zirconium dichloride was prepared by previous members in Chung's group at Penn State using a previously reported method.¹¹ 1,4-Polybutadiene (Avg. Mw = 420,000 g/mol) was dissolved in tetrahydrofuran (THF), precipitated in methanol and vacuum dried prior to use. Two poly(vinyl alcohol-co-ethylene) copolymers, having 38 and 44 mol % ethylene respectively, obtained from Sigma-Aldrich Co., were dissolved in water/n-propanol (1:1) mixture, precipitated and dried under vacuum at 100 °C for 12 hours prior to use. Two polyvinyl alcohols, 87-89 % and 98-99 % hydrolyzed, respectively (Both avg. Mw = 88,000-97,000 g/mol), purchased from Alfa Aesar, were dissolved in dimethylformamide (DMF), precipitated in isopropanol, and dried under vacuum at 130 °C for 12 hours prior to use. Hexenyl-9-BBN was synthesized by a previously reported method.^{12,13}

Commercial capacitor grade isotactic polypropylene (EM 4342C2, EM iPP), obtained from ExxonMobil Chemical, and commercial branched high melt strength polypropylene (Daploy WB135HMS, HMS), obtained from Borealis, were used without further purifications.

^1H nuclear magnetic resonance (NMR) spectra were obtained using a Bruker AM 300 NMR at 110 °C. Purified polymers were dissolved in good solvent, 1,1,2,2-tetrachloroethane- d_2 for PP-OH and dimethyl sulfoxide- d_6 for others, and scanned until the desired signal-to-noise ratio was obtained.

Electrical polarization was measured using an automated polarization measurement system provided at Penn State. Prior to the polarization measurement, 3-mm diameter gold electrodes were sputtered on each side of a sample film. The film with deposited electrodes was loaded onto a sample holder, and electric field increments of 50 MV/m were applied at 10 Hz. The applied field was increased until the film failed.

The dielectric constants of polypropylene-butyl-OH (PP-OH), commercial biaxially oriented polypropylene films and poly(vinyl alcohol-co-ethylene) (PVA-co-PE) were measured using an HP multifrequency LCR meter (HP 4284A) in the frequency range 20 to 200 kHz. Data points were collected every 2 °C while heating at 2 °C/min. Temperature ranges covered were 0-120 °C for PP-OH and commercial films, and -100 to 120 °C for the PVA-co-PE copolymers. The dielectric constants of the remaining samples were measured using a Novacontrol GmbH Concept 40 broadband dielectric spectrometer in order to study the temperature/frequency dependence of these films in greater detail. The frequency range covered was 0.01 to 10 MHz. Data points were isothermally collected every 5 °C in the range -100 to 110 °C (within ± 0.5 °C of the set point). Samples were purged by dry N_2 throughout the measurements to minimize the effects of water.

A Seiko DSC220CU differential scanning calorimeter (DSC) was used to obtain glass transition temperatures (T_g) and melting temperatures (T_m). In each run, the sample was initially heated from 10 °C below the expected T_g to 20 °C above the expected T_m at 10 °C/min, held isothermally for 3 min, cooled down to the initial temperature at 40 °C/min, then heated at 10

°C/min. T_g and T_m were determined from the second heating scan to eliminate effects from prior processing.

3.2.2 Copolymerization of Propylene and Hexenyl-9-BBN

100 ml of dry toluene and 5 ml of MAO were added into a dry 450 ml Parr stainless steel autoclave equipped with a mechanical stirrer. The reactor was heated up to 35 °C. 1.4×10^{-2} moles of hexenyl-9-BBN was introduced to a stirring autoclave, followed by 3.0×10^{-6} moles of $\text{rac-Me}_2\text{Si}_2\text{ZrCl}_2$ catalyst solution and 60 psi of propylene monomer. Monomer was continuously fed while maintaining the reactor temperature at 35 °C. The reaction was terminated after 1.5 h using methanol.

3.2.3 Oxidation Reaction of Polypropylene-butyl-9-BBN Copolymers

The still wet polypropylene-butyl-9-BBN copolymer was rinsed with acetone and put into a 2 L three-neck, round-bottom flask equipped with a magnetic stir bar along with 100 ml THF. A condenser connected to an argon gas line was mounted onto one of the necks of the round bottom flask. The other two necks were capped with rubber septa. 165 g of 30 % hydrogen peroxide and 200 ml of THF were put into a 500 ml round bottom flask. In another 500 ml flask, 22.5 g sodium hydroxide and 75 ml of distilled water were introduced. All three flasks were purged with argon gas for 1 hour. The 2 L flask was immersed in an ice bath and the sodium hydroxide–water solution was introduced. After 10 min stirring, the hydrogen peroxide–THF solution was also introduced dropwise. After the hydrogen peroxide-THF solution was completely added, the 2 L flask was warmed to room temperature and stirred over night at 40 °C. The product was precipitated by water. The procedure of dissolution and crystallization in boiling

toluene followed by washing in warm water was repeated two times. After the purification, the product was dried in a vacuum oven at 85 °C for 12 hours.

3.2.4 Functionalization of 1,4-Polybutadiene

10 g of 1,4-polybutadiene was introduced into a 2 L three-neck, round-bottom flask equipped with a magnetic stir bar. A condenser connected to an argon gas line was mounted onto the flask. The other two necks were capped with rubber septa. The flask system was vacuum pumped for 30 min. 410 ml of 0.5 M 9-BBN in THF was introduced to the 2 L flask with positive pressure and stirred for 5 h at 40 °C. 245 g of 30 % hydrogen peroxide and 210 ml of THF were put into a 500 ml round bottom flask. In another 500 ml flask, 57.3 g sodium hydroxide and 185 ml of distilled water were introduced. All three flasks were purged with argon gas for 1 hour. While keeping the 2 L flask ice-cool, the sodium hydroxide–water solution was introduced. After 10 min stirring, the hydrogen peroxide–THF solution was also introduced dropwise. After all of the hydrogen peroxide-THF solution was added, the 2 L flask was warmed to room temperature and stirred over night at 40 °C. The polymer product was precipitated with water. The procedure of dissolution and crystallization in good solvent followed by washing in warm water was repeated two times. The product was dried in a vacuum oven at 90 °C for 12 hours.

3.2.5 Thin Film Preparation

Solution casting or melt pressing were both utilized and the conditions were selected specifically for the sample processed to minimize the residual solvent and possible crosslink formation. The general guidelines for film preparation were: All polypropylene-butyl-OH polymers, 1,4-polybutadiene with 50, 75 and 100 % OH functionalization, and poly(vinyl

alcohol-co-ethylene) with 38 and 44 mol % ethylene content were melt pressed by a Carver Inc. hydraulic press between Teflon sheets at 180, 140, 150, 170, and 180 °C, accordingly. Preheating time without pressure and pressing time were varied between 1.5 to 5 min each depending on the sample used. Unmodified 1,4-polybutadiene was dissolved in THF and solution cast onto a brass electrode, dried in air, and annealed under vacuum at 70 °C for 6 hours. Poly(vinyl alcohol-co-ethylene) with 38 and 44 mol % ethylene films prepared for polarization measurements and polyvinyl alcohol with 88 % and 99 % hydrolyzation were dissolved in DMF and solution cast. Prepared films were dried in a vacuum oven at 135 °C for 8 hours. All of the samples except the unmodified 1,4-polybutadiene were gold sputtered. The procedure of 10 sec sputtering and 1.5 min cooling was repeated 15 times per side to have 2.5 min total sputtering time a side. The electrode sizes and shapes used in different measurements were 3 mm diameter circles for polarization measurements, and 7 mm or 1 cm diameter circles for all the dielectric constant measurements with the exception of unmodified 1,4-polybutadiene.

3.3 Hydroxylated Polypropylene (PP-OH) Dielectric Properties

Currently available commercial polypropylene capacitor films have higher breakdown strength than other polymer based film capacitors. Despite its commercial success, the total energy density stored on a commercial polypropylene capacitor is about 1 to 1.2 J/cm³, which is roughly half of a polyvinylidene fluoride (PVDF) film, 2.4 J/cm³.¹ The low energy storage capability of a polypropylene film is attributed to its low dielectric constant, 2.5. It is, therefore, essential to increase the dielectric constant of a polypropylene film through functionalization with a polar group. The dielectric properties of hydroxylated polypropylene (PP-OH) are discussed in this section.

3.3.1 Dielectric Constant of PP-OH Polymers

Table 3-1 summarizes the hydroxylated polypropylene (PP-OH) synthesis with various OH concentrations in the samples. Note that the catalyst reactivity was greatly affected by the concentration of hexenyl-9-BBN comonomer used. The dielectric spectra of a commercial biaxially oriented polypropylene (BOPP) film and hydroxylated polypropylene samples at 2 kHz are shown in Figure 3-1.

Table 3-1: Comparison of hydroxylated polypropylene with various OH concentrations.

	Solvent (ml)	Comon. (mmol)	Propylene (psi)	Rxn. Time (h)	Rxn. Temp (°C)	Yield (g)	[OH] (mol %)	Mv (g/mol)	T _g (°C)	T _m (°C)
PP-OH 1	150	7	128	1.5	40	12.45	0.12	247,500	-1	157
PP-OH 2	150	7	60	1.5	35	3.77	0.34	206,500	0	149
PP-OH 3	150	21	60	1.5	35	2.83	1.74	156,900	4	134

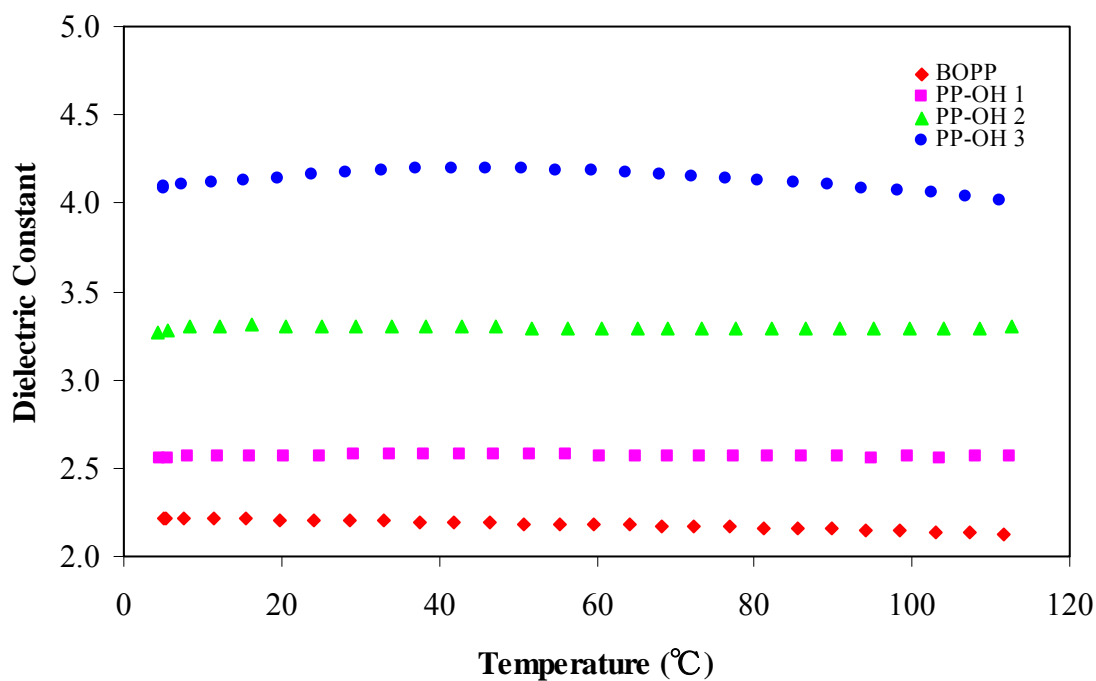


Figure 3-1: Dielectric constant of BOPP and PP-OH at 2 kHz.

The dielectric constant of BOPP film was about 2.3. With merely 0.12 mol % of functionalization, the dielectric constant increased to 2.5 in PP-OH 1, and it was further increased to 4.1 with 1.74 mol % OH content in PP-OH 3. The dielectric constants of PP-OH 1 and 2 showed temperature or frequency independent behaviors (Figure 3-1). However, a trace of fluctuation in the dielectric constant was observed in PP-OH 3, where the peak was around 40 °C. This change indicates that polarization in PP-OH 3 is not only due to induced polarization, but also due to dipole polarization. It also suggests that further incorporation of hydroxyl group would intensify the dielectric peak.

Using the dielectric constants obtained from the BOPP and PP-OH samples, the theoretical energy density of the polymers under several hypothetical conditions were calculated. The calculation results are summarized in Table 3-2. Based on the estimation, a commercial 10 μm BOPP film would have an energy density of at least 2.5 J/cm^3 , as its typical breakdown strength is greater than 600 MV/m. The energy density is expected to double if PP-OH 3 could withstand the applied field of 500 MV/m. The same effect could be achieved under low electric field if the dielectric constant of PP-OH can be improved further. In order to achieve the maximum energy, however, it is crucial that all of the relevant factors are optimized. The desirable conditions include a high dielectric constant ($\epsilon > 5$), reduced thickness ($d < 10 \mu\text{m}$), and high breakdown strength ($E > 500 \text{ MV/m}$).

Table 3-2: Theoretically estimated energy density of BOPP and PP-OH.

	Dielectric constant (ϵ)	Film thickness (μm)	Applied voltage (kV)	Applied field (MV/m)	Energy density (J/cm^3)
PP	2.3	20	5	250	0.6
	2.3	10	5	500	2.5
PP-OH 1	2.6	20	5	250	0.7
	2.6	10	5	500	2.9
PP-OH 2	3.3	20	5	250	0.9
	3.3	10	5	500	3.7
PP-OH 3	4.3	20	5	250	1.2
	4.3	10	5	500	4.8

3.3.2 Polarization Loops of PP-OH Polymers

Hydroxylation of polypropylene increased the dielectric constant by 85 % with incorporation of merely 1.7 mol % of hydroxyl groups. While this improvement was encouraging, a capacitor is operated under much higher electric fields than those used in the dielectric experiments. It is essential to investigate the polarization-depolarization curves of the PP-OH polymers under high electric fields. Polarization curves of EM, HMS and PP-OH films in three thickness ranges are shown in Figure 3-2.

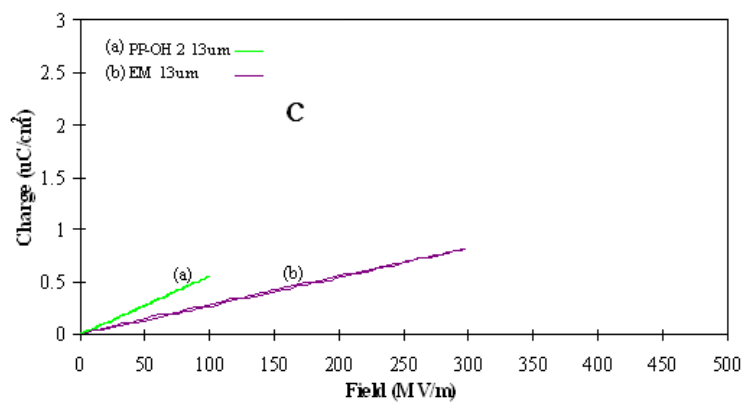
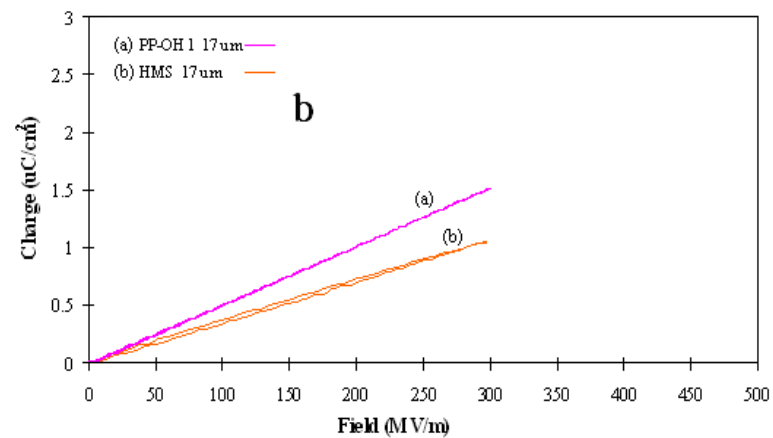
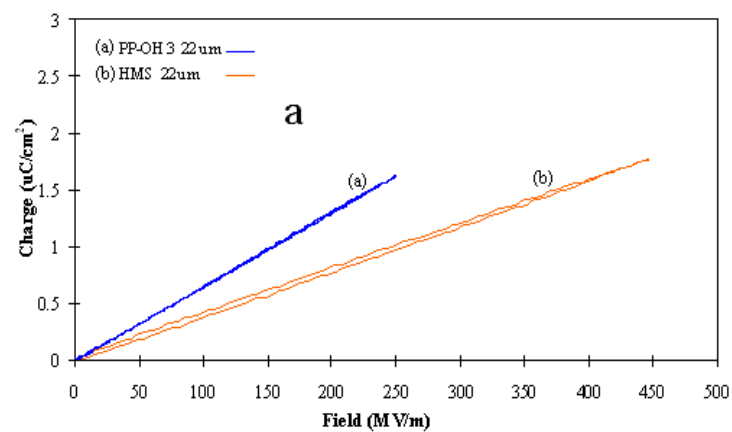


Figure 3-2: Polarization-depolarization curves of PP-OH and non-functionalized polypropylene derivatives: (a) PP-OH 3, 22 μm, (b) PP-OH 1, 17 μm, and (c) PP-OH 2, 13 μm.

Polarization-depolarization curves of these samples were all linear as the predominant polarization in these samples was attributed to induced polarization. The PP-OH samples contained a polar group, which introduced dipole polarization, yet no change in the shape of the polarization curves was observed due to the low concentration of the hydroxyl group.

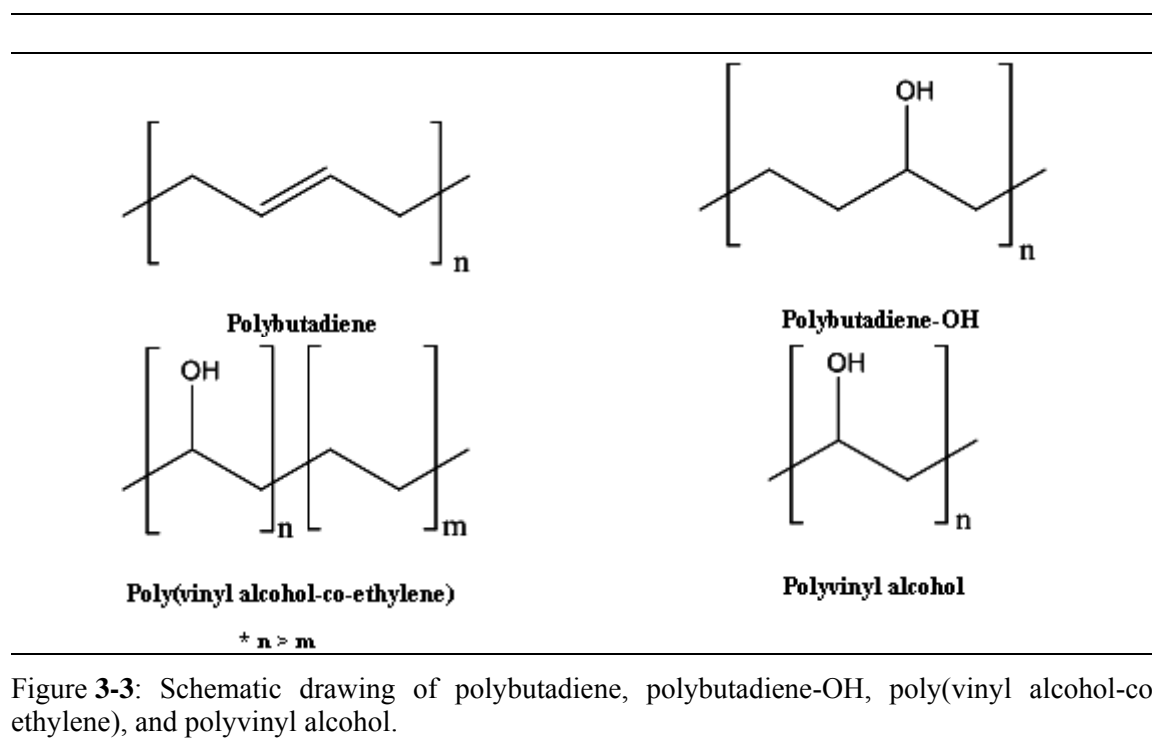
A 62 % increase in the polarization slope was observed with 1.74 mol % functionalization in PP-OH 3, relative to HMS (Figure 3-2 (a)). The increase in the slope of PP-OH 1 was 43 % at 17 μm compared to HMS with the equivalent thickness (Figure 3-2 (b)). The effect of functionalization was most prominent in Figure 3-2 (c), where the slope of PP-OH 2, the sample with 0.34 mol % OH group, increased by 97 % relative to the non-functionalized EM sample.

Improvement in the overall film quality is crucial for the further detailed systematic studies. Nevertheless, comparisons of the polarization slopes of various functionalized and unfunctionalized samples with equivalent thicknesses demonstrated the benefits of functionalization.

3.4 Hydroxylated Polymer Dielectric Spectroscopy

Hydroxylation of polypropylene showed changes in the dielectric constant, and the effect became more prominent with the increase in the degree of functionalization. While further -OH incorporation was desirable, it was practically infeasible due to the rapid reduction in the catalyst reactivity with increasing comonomer concentration. As an alternative approach, 1,4-polybutadiene was modified to create an alternating copolymer of -CH₂-CH₂- and -CHOH-CH₂- units. Degrees of modification were 50, 75 and 100 %, and the samples were labeled PB-OH 50, 75, and 100, respectively. Complete conversion of double bonds to hydroxyl groups gave the alternating copolymer, while partial conversion resulted in a random terpolymer with -CH₂-CH₂-,

-CH₂-CH=CH-CH₂- and -CHOH-CH₂- units. In addition to the modified 1,4-polybutadiene, poly(vinyl alcohol-co-ethylene) with 38 and 44 mol % ethylene and polyvinyl alcohols (PVA 62 and 56, respectively), 87 to 89 % and 98 to 99 % hydrolyzed (PVA 88 and 99, respectively), were analyzed. These samples covered the entire spectrum of hydroxylation from unmodified polybutadiene to a functionalization of 99 % hydrolyzed polyvinyl alcohol. Structures of the polymers studied in this section are illustrated in Figure 3-3.



3.4.1 Dielectric Constant of Hydroxylated Polymers

Dielectric spectra of the samples are shown in Figure 3-4, and the glass transition temperatures (T_g) of the hydroxylated polymers are in Table 3-3. The dielectric constant of 1,4-polybutadiene was about 2.5, which is similar to that of a commercial polypropylene film, 2.3. A 50 % functionalized polybutadiene indicated the presence of peaks in the dielectric constant. The

effect of the hydroxylation, however, was small compared to the dielectric constant of PP-OH 3 obtained in the previous section. Despite the difference in the OH content, the difference in the dielectric constant of PP-OH 3 and PB-OH 50 was small, 4.3 and 4.4 at 200 Hz, respectively. The hydroxyl content in PB-OH 50 was about 10 times greater than that of PP-OH 3. One explanation of the relatively high dielectric constant of PP-OH 3 is the mobility of the hydroxyl group. As previously mentioned, the OH group in PP-OH 3 was attached to the end of butyl branch, while the OH in PB-OH 50 was attached directly to the polymer backbone. During a dielectric constant measurement, the hydroxyl groups in the samples were poled by a low voltage, which helped to separate charges on the surface of the electrodes. The relatively high dielectric constant of PP-OH 3 was attributed to the better orientation of the hydroxyl group along the applied electric field.

Table 3-3: General compositions and properties of PB-OH and PVA polymers.

	[OH] ^a	T _g (°C)	T _m (°C)
PB-OH 50	1/8	1	-
PB-OH 75	1/5.3	34	-
PB-OH 100	1/4	50	-
PVA 56	1/3.6	57	160
PVA 62	1/3.2	63	173
PVA 88	1/2.3	69	192
PVA 99	1/2	78	213

a. OH concentration: 1 OH/ # of carbons in the backbone

With the increase in the hydroxyl functionalization, the dielectric constant was also increased. The peak of PB-OH 75, 12.1, which improved from 4.4 of PB-OH 50, was further increased to a dielectric constant of 24.5 in PB-OH 100 at 20 Hz. Compared to the starting polybutadiene, the dielectric constant was increased nearly an order of magnitude with the hydroxyl group in every repeating unit. The functionalization not only improved the dielectric constant, but it also increased the temperature at which the peaks in the dielectric constant occurred. The locations of the peak range shift from 25 to 60 °C, 40 to 70 °C, to 50 to 80 °C, as the OH content increased in PB-OH 50, 75, 100, respectively. The difference in the locations of

the temperature range was influenced by T_g , which increased with the higher degree of modification.

The PB-OH 100 polymer containing alternative vinyl alcohol and ethylene units in the backbone shows dielectric constant $\epsilon \approx 30$ at 50 °C and 20 to 200 Hz, indicating the parallel OH dipole orientation. In addition, the peaks in the dielectric constant of PB-OH 100 are within the optimum operating temperature range of commercial capacitors, 60 °C. This suggests that PB-OH 100 would exhibit its best performance under a practical application condition, and makes it a favorable material for the film capacitor application.

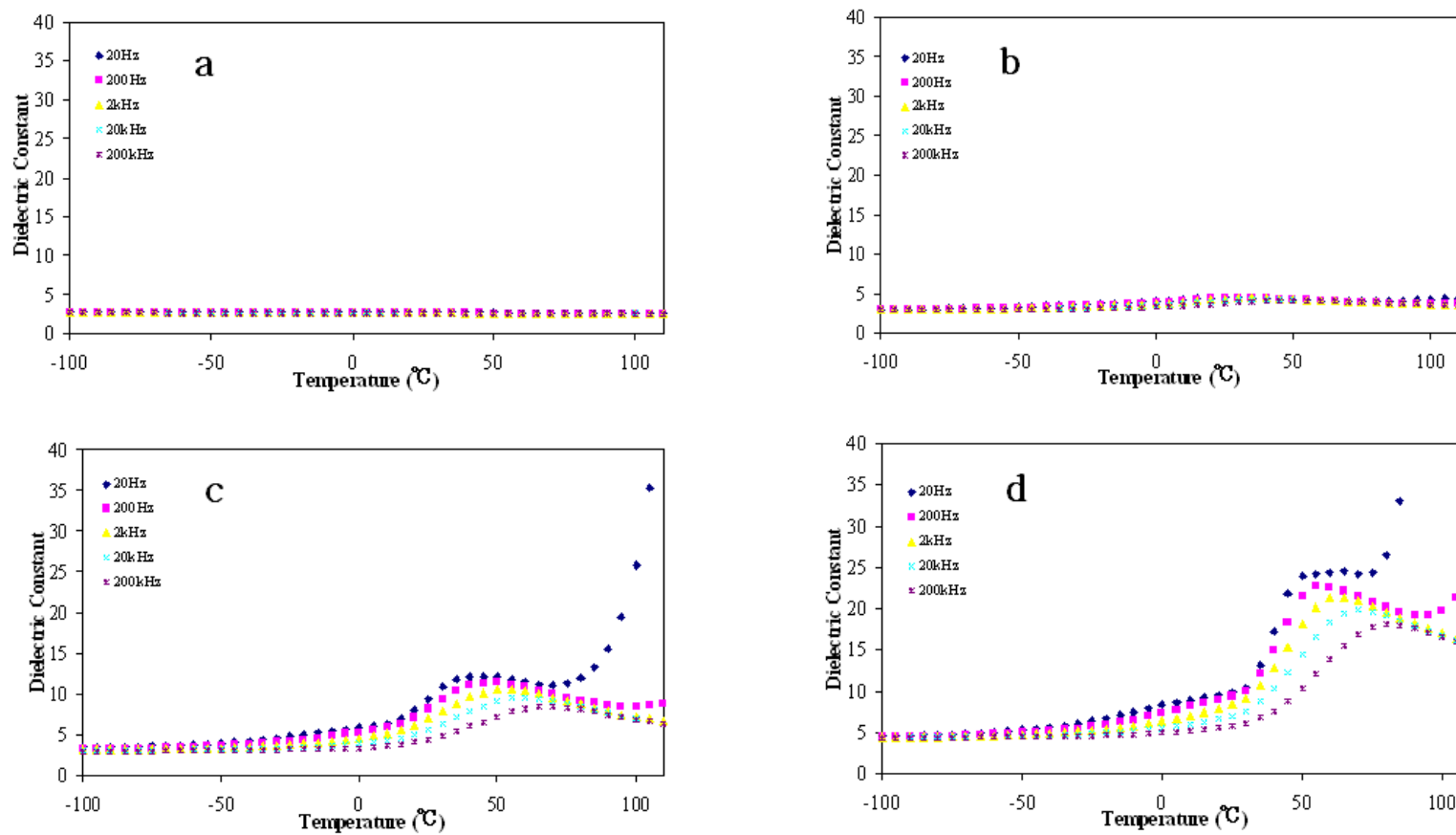


Figure 3-4: Dielectric constant vs temperature spectra of (a) polybutadiene, (b) PB-OH 50, (c) PB-OH 75, and (d) PB-OH 100.

The complete functionalization of polybutadiene incorporated one hydroxyl group in every four backbone carbons, including one unit of $-\text{CH}_2\text{-CH}_2-$ as a spacer. The effect of further incorporation of OH groups on the dielectric constant was investigated using commercial PVA 56, 62, 88, and 99. Two PVA 56 and 62 are structurally similar to previously studied PB-OH samples, except the repeating unit with $-\text{CH}_2\text{-CH}_2-$ and $-\text{CH}_2\text{-CHOH-}$ are randomly ordered. On the other hand, PVA 88 and 99 have the repeating unit of $-\text{CH}_2\text{-CHOH-}$, where the unhydrolyzed portion has $-\text{O-C(=O)CH}_3$ instead of OH. With no $-\text{CH}_2\text{-CH}_2-$, PVA 99 has double the concentration of hydroxyl groups compared to 100 % modified PB-OH. Dielectric constants of the samples are shown in Figure 3-5.

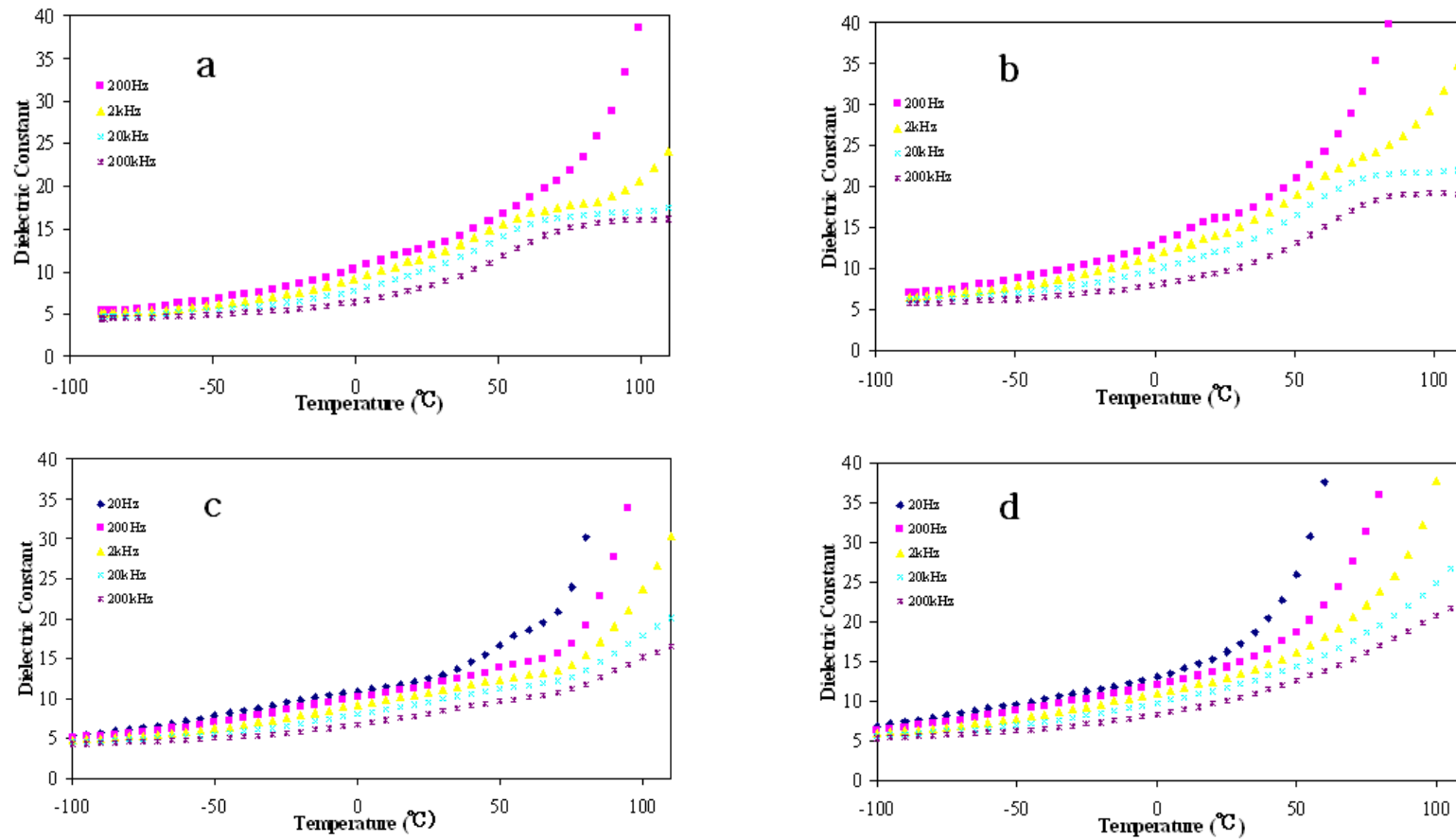


Figure 3-5: Dielectric constant vs temperature spectra of (a) PVA 56, (b) PVA 62, (c) PVA 88, and (d) PVA 99.

The shift of dielectric constant peaks to higher temperatures is similar to what was observed previously for the modified polybutadiene. The actual intensity of the peaks, however, was not clear as the dielectric constant rapidly increases at high temperatures in every sample, particularly in PVAs. The high dielectric constant observed at the high temperature region was due to the high mobility of free ions. The hydroxyl groups present at high concentration moved readily above the T_g of the samples, and no clear dielectric constant peak attributed solely due to the polarization of OH groups was observed.

While the effect of the free ions was apparent at low frequencies, traces of high-frequency peaks were present in PVA samples. Comparing PB-OH 100 and PVA 56, whose OH contents were about the same, their near peak dielectric constants at 20 kHz were 19.8 and 16.7, accordingly. In this case, the increase in the hydroxyl content reduced the dielectric constant. The decrease in the dielectric constant was attributed to the structural differences of the samples. As previously explained, the hydroxyl groups of PB-OH 100 were separated by $-\text{CH}_2-\text{CH}_2-$. In the case of PVA 56 random copolymer, it is possible that multiple $-\text{CH}_2-\text{CHOH}-$ units were located adjacent to each other. When two hydroxyl groups are in close proximity, a hydrogen bond forms between them. Not only would this bond lead to the possible cancellation of dipoles, but extra energy is required to dissociate the bond and this delays the response of the hydroxyl groups to the electric field. Elevated temperatures provided the energy required for the dissociation of the hydrogen bonds. At these temperatures, however, sufficient energy is also provided to allow for the movement of the free ions. As a result, no clear dielectric constant peaks were observed in the two PVA 56 and 62 samples.

The theoretical energy densities of these hydroxylated polymers under several hypothetical conditions were calculated by the same procedure used in Section 3.3.1 for PP-OH. Table 3-4 summarizes the calculated results.

Table 3-4: Theoretically estimated energy density of polybutadiene and PB-OH samples at 20 Hz.

	Dielectric constant (ϵ)	Film thickness (μm)	Applied voltage (kV)	Applied field (MV/m)	Energy density (J/cm^3)
Polybutadiene	2.6	20	5	250	0.7
	2.6	10	5	500	2.9
PB-OH 50	4.4	20	5	250	1.2
	4.4	10	5	500	4.9
PB-OH 75	12.1	20	5	250	3.3
	12.1	10	5	500	13.4
PB-OH 100	24.5	20	5	250	6.8
	24.5	10	5	500	27.1

PVA-co-PE and PVA samples were omitted, as it was difficult to isolate the dielectric constant peak in these samples. When the dielectric constant increased nearly an order of magnitude in PB-OH 100 compared to the unmodified polybutadiene, the energy density also increased remarkably. The energy density of a 10 μm polypropylene film under an applied field of 500 MV/m is 2.9 J/cm^3 , as previously calculated in Section 3.3.1. The calculated energy density of PB-OH 100 easily exceeds this, and it would have an energy density of 6.8 J/cm^3 even at a lower electric field, 250 MV/m. The goal is to achieve an energy density of 27.1 J/cm^3 at 500 MV/m. Nevertheless, it is encouraging that these samples may give the high energy density even at a lower applied field.

Another essential property of a capacitor material is its reversibility. A capacitor generates heat when under operation, even with the presence of a cooling system. It is therefore necessary to check whether the dielectric constant remains the same during a heating-cooling cycle. Heating-cooling scans of the selected samples at 2 kHz are shown in Figure 3-6.

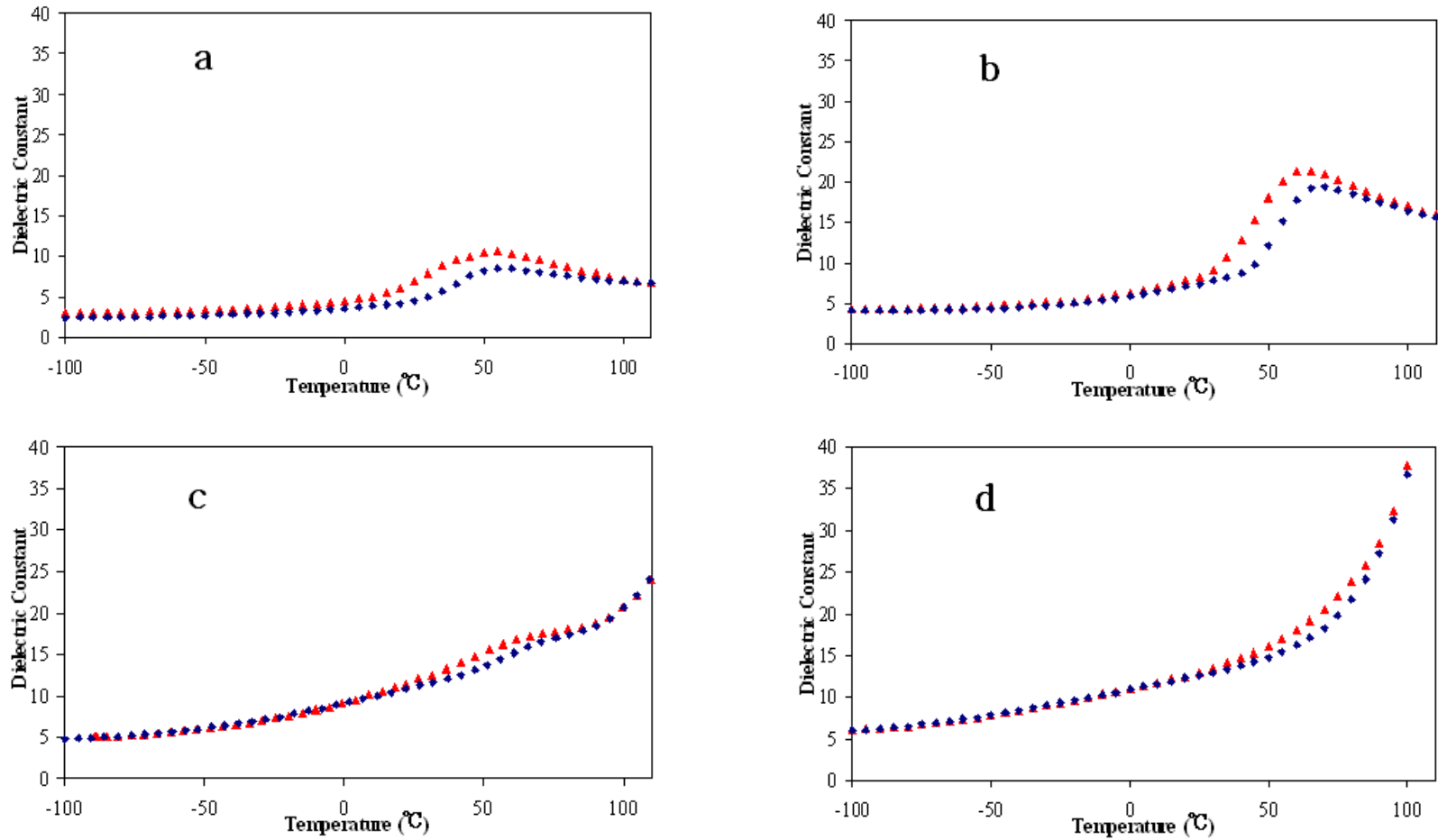


Figure 3-6: Dielectric constant vs temperature spectra of (a) PB-OH 75, (b) PB-OH 100, (c) PVA 56, and (d) PVA 99 in heating-cooling scans at 2 kHz. The red triangles represent the heating scan and the blue squares represent the cooling scan.

At elevated temperatures, above 100 °C, no difference in the dielectric constant was observed in the heating and cooling cycle. At lower temperatures, specifically in the vicinity of the peak in the dielectric constant, a difference between the heating and cooling scans was observed. Compared to the heating scan, the peak in the dielectric constant in the cooling cycle appeared to have decreased in magnitude and shifted to higher temperatures. This change in the cooling cycle may be attributed to the change in the segmental relaxation, where the hydroxyl groups were induced to align along the electric field during the heating scans. The shift of the dielectric constant peak indicates that the heating scan may be a more accurate representation of the dielectric properties of the materials than the cooling cycle.

3.4.2 Polarization-depolarization Curves of Hydroxylated Polymers

Polarization-depolarization curves of hydroxylated polymers were measured. PB-OH 50 and 75 were not measured due to their softness and difficulties in processing into stable films. For other samples, polarization loops were measured at room temperature. The results are shown in Figure 3-7.

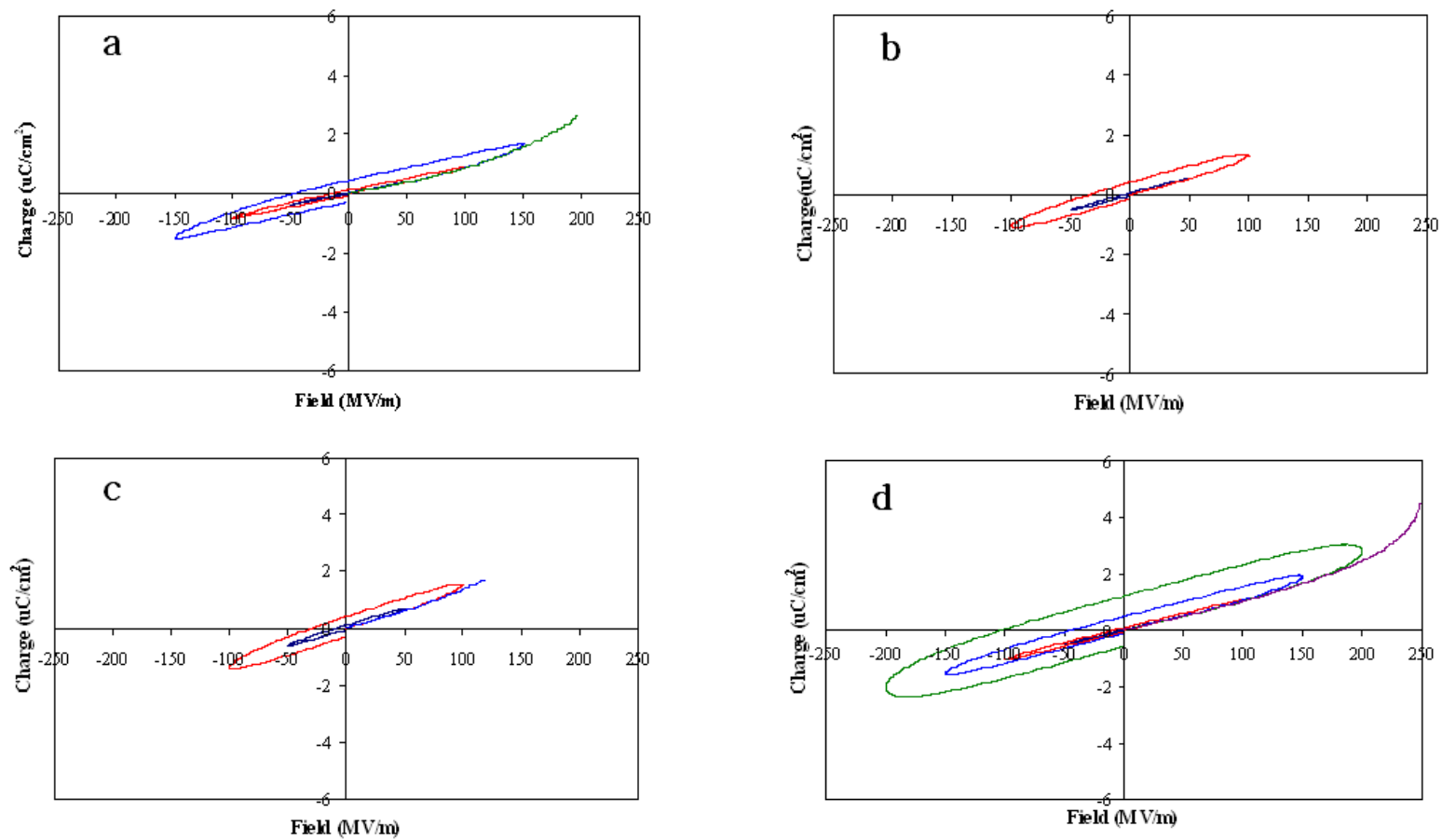


Figure 3-7: Polarization-depolarization curves of (a) PB-OH 100, 17 μm , (b) PVA 56, 17 μm , (c) PVA 62, 16 μm , and (d) PVA 88, 17 μm . Measured at room temperature.

A trend in the polarization slopes was observed: they initially increased with increasing concentration of the hydroxyl group. However, the slope decreased in PVA 88. These changes resulted from the combination of T_g and hydroxyl content of the samples. At room temperature, the hydroxyl groups in all the measured samples were immobile as it was below their T_g . Under this condition, the structures with a higher content of hydroxyl groups would induce greater permittivity. However, when the distance between each hydroxyl group is sufficiently short, as represented by PVA 88, the OH groups form hydrogen bonds which disrupt the charge distribution in the polymer matrix. This resulted in the reduction of the slope.

In the polarization loops of the hydroxylated polymers, energy loss was observed, particularly among the samples with a higher content of OH group. As a general trend, the energy loss and irreversibility in the bipolar polarization measurement became more prominent with an increasing applied electric field. It is interesting to note that in both the polarization and depolarization phases, the slope of the curves changes linearly, while that of fluoropolymers changes nonlinearly during a polarization-depolarization cycle. The linear change of the slopes and irreversibility of the curves may suggest that the polarizations observed in Figure 3-7 can be attributed to the induced and forced-dipolar polarizations. As indicated in Table 3-3, the T_g of the measured samples was much higher than room temperature. When the films are placed under an electric field, polarization is induced. The slope remains linear as this polarization is due to the change in the charge distributions in the $-CH-CH_3$ and $-CH-OH$ groups. Under a higher electric field, sufficient energy is provided to pole the hydroxyl groups along the field. This may be why a slight increase in the slope of the polarization curve was observed at high breakdown strength. During depolarization, the poled hydroxyl group cannot go back to its original state due to kinetic trapping. As a result, the OH groups are frozen at the half-polarized state and discharged without going back to the original state.

As an extension of the study, polarization loops of the samples were also measured at 50 °C. However, low breakdown strength (<100 MV/m) and unusually large energy loss were observed. Higher quality, defect-free films must be prepared and used in future trials to obtain a detailed understanding of the hydroxylation effect on the polarization curves at elevated temperatures.

The effect of hydroxylation on the slopes of polarization curves was assessed by comparing the slopes of the hydroxylated polymers and a 12 μm commercial polypropylene film. The polarization-depolarization curve of a commercial BOPP in section 1.4.4 showed that the charge density of the film reached 2 $\mu\text{C}/\text{cm}^2$ with a breakdown strength of 700 MV/m. PB-100 and PVA 88 reached the same charge density at 150 MV/m, while PVA 56 and 62 samples were at 100 MV/m. Simply calculated, this indicates that the hydroxylation increased the slope by a factor of 4.7 in PB-100 and PVA 88, and 7 in PVA 56.

3.5 Conclusions

The effect of hydroxylation on the dielectric response of a non-polar polyolefin was studied. Two types of functionalized structures were prepared, one where the hydroxyl group was attached to the end of butyl side chains and one where the hydroxyl group was directly attached to the polymer backbone.

Compared to a commercial polypropylene film, propylene-hexenyl-OH 3 showed an 85 % increase in permittivity with a functionalization of only 1.7 mol %. In the polarization study, PP-OH 2 almost doubled the slope of the polarization curve with 0.34 mol % functionalization, though its breakdown strength needed to be improved.

Effects of further functionalization with the OH group were studied. The samples used in this study had the hydroxyl groups directly attached to the polymer backbones, and this reduced

the mobility of hydroxyl groups relative to the other functionalized structures. Comparative studies of PP-OH, PB-OH, PVA-co-PE and PVA showed that the dielectric constant is not only dependent on the concentration of the incorporated polar groups, but also on the structure of the polymer. High mobility and minimum interaction with other polar groups are two essential factors in the maximization of the peak in the dielectric constant. In order to achieve these, an alternating copolymer or a homopolymer with spacer groups between each functional group is desirable. This prevents the formation of hydrogen bonds and ensures the high mobility of the hydroxyl groups.

Dielectric spectra showed changes in the peak of the dielectric constant where it shifted to higher temperatures and decreased in magnitude. Among the hydroxylated polymers, PB-OH 100 showed the greatest increase in dielectric constant, 24.5, nearly an order of magnitude higher than the dielectric constant of polypropylene, 2.5. In addition, the peaks in the dielectric constant of PB-OH 100 were in the desirable temperature range, 50 to 80 °C. The optimum operation temperature of large scale commercial capacitors is around 60 °C. It is, therefore, encouraging that the highest dielectric constant in the tested samples was achieved in the optimum operating temperature. Also in this temperature range at 20-200 Hz, PB-OH 100 indicated the parallel OH dipole orientation.

Polarization-depolarization loops of the hydroxylated polymers showed improvement in their slopes. The slope and energy loss were dependent on T_g and hydroxyl group content. Further improvement in the film quality is crucial in understanding the hydroxylation effects on the polarization curves in greater detail.

References

1. Rabuffi, M.; Picci, G., Status quo and future prospects for metallized polypropylene energy storage capacitors. *Plasma Science, IEEE Transactions on* **2002**, 30, (5), 1939-1942.
2. Tressaud, A.; Durand, E.; Labrugère, C.; Kharitonov, A. P.; Kharitonova, L. N., Modification of surface properties of carbon-based and polymeric materials through fluorination routes: From fundamental research to industrial applications. *Journal of Fluorine Chemistry* **2007**, 128, (4), 378-391.
3. Kharitonov, A. P., Practical applications of the direct fluorination of polymers. *Journal of Fluorine Chemistry* **2000**, 103, (2), 123-127.
4. Zhenlian, A.; Min, Z.; Junlan, Y.; Yewen, Z.; Zhongfu, X., Influence of fluorination on piezoelectric properties of cellular polypropylene ferroelectrets. *Journal of Physics D: Applied Physics* **2009**, (1), 015418.
5. Cheng, Z.; Zhang, Q.; Su, J.; Tahchi, M. E., Electropolymers for Mechatronics and Artificial Muscles. In *Piezoelectric and Acoustic Materials for Transducer Applications*, 2008; pp 131-159.
6. Zhang, Z.; Chung, T. C. M., Study of VDF/TrFE/CTFE Terpolymers for High Pulsed Capacitor with High Energy Density and Low Energy Loss. *Macromolecules* **2007**, 40, (4), 783-785.
7. Chung, T. C.; Petchsuk, A., Synthesis and Properties of Ferroelectric Fluoroterpolymers with Curie Transition at Ambient Temperature. *Macromolecules* **2002**, 35, (20), 7678-7684.
8. Chung, T. C.; Rhubright, D., Synthesis of functionalized polypropylene. *Macromolecules* **1991**, 24, (4), 970-972.
9. T. C. Chung, D. R., Functionalization of polypropylene by hydroboration. *Journal of Polymer Science Part A: Polymer Chemistry* **1993**, 31, (11), 2759-2763.
10. Chung, T. C.; Janvikul, W., Borane-containing polyolefins: synthesis and applications. *Journal of Organometallic Chemistry* **1999**, 581, (1-2), 176-187.
11. Spaleck, W.; Kueber, F.; Winter, A.; Rohrmann, J.; Bachmann, B.; Antberg, M.; Dolle, V.; Paulus, E. F., The Influence of Aromatic Substituents on the Polymerization Behavior of Bridged Zirconocene Catalysts. *Organometallics* **1994**, 13, (3), 954-963.
12. Brown, H. C.; Liotta, R.; Kramer, G. W., Hydroboration. 49. Effect of structure on the selective monohydroboration of representative conjugated dienes by 9-borabicyclo[3.3.1]nonane. *The Journal of Organic Chemistry* **1978**, 43, (6), 1058-1063.
13. Chung, T. C.; Raate, M.; Berluce, E.; Schulz, D. N., Synthesis of functional hydrocarbon polymers with well-defined molecular structures. *Macromolecules* **1988**, 21, (7), 1903-1907.

Chapter 4

Conclusions and Suggestions

4.1 Summary of Present Work

Potential improvements in the processibility and material dielectric properties of polypropylene capacitors were explored. The dependence of the LCB to styrene ratio was examined. Ratios of high temperature reactions (above 37 °C) were equal or below 1 in every case and showed no dependence on the reaction conditions. Contrarily, an increase in the ratio was observed in low temperature reactions (below 37 °C). Increase in the ratio of branch/styrene group may be due to the stability of the dormant catalyst site, resulting from the chain transfer of growing polymer chains to the pendant styrene groups. It is possible that the structure with the dormant catalyst site is stable, which makes the chain transfer of growing polymer chains to the pendant styrene group a kinetically favorable termination for the growing polymer chains rather than the termination by β -hydride elimination. Perhaps this may have helped to form more long chain branches relative to the styrene group.

BSt consumption was improved through a two-step synthesis of a long chain branched polymer having polyethylene backbone and polypropylene side chains (PE-BSt-PP). The degree of consumption of BSt in a PE-BSt copolymerization was as high as 100 % when 0.1 g of BSt was used. The PE-BSt was further copolymerized with propylene to synthesize PE-BSt-PP. A high degree of styrene consumption, 77-100 %, was achieved and 0.03-0.01 mol % of branches was formed.

The breakdown strength of commercial linear and branched polypropylene, and long chain branched polypropylene prepared via the T-reagent was assessed. Better Weibull alpha and beta values were obtained from the samples with a high branch density. The high statistical

stability of the breakdown strength may be attributed to the continuous network of polymer chains formed by the long chain branches, where the entanglement of polymer chains increased the qualitative uniformity within a film and reduced fatal defects than the linear sample. The relatively high alpha and beta values were encouraging as the improvement in the film quality would further improve the values.

Another important property of a capacitor film, permittivity, was improved through hydroxylation. The hydroxyl groups were attached to the end of butyl side chains which were incorporated in the polypropylene backbone. The dielectric constant increased by 65 % even with low concentration of hydroxyl groups (1.74 mol %). Hydroxyl content was further increased and examined using modified 1,4-polybutadiene, poly(vinyl alcohol-co-ethylene) and polyvinyl alcohol. Permittivity was increased by an order of magnitude at 100 % hydroxylation of 1,4-polybutadiene, PB-OH 100. A dielectric constant of 24.5, similar to the estimated dielectric constant of 30, was obtained from PB-OH 100 at 50 °C and 20 to 200 Hz. This sample is desirable not only due to its improved dielectric constant but also due to the temperature shift of the dielectric constant peaks. The optimum capacitor operating temperature in practical applications is around 60 °C, and the peak in the dielectric constant of PB-OH 100 was in the 50-80 °C range, depending on the chosen frequency. This indicates that OH groups are oriented parallel to the electric field, and the film demonstrates its best performance at the typical operating temperature of commercial capacitors.

The dielectric constant studies of the hydroxylated polymers also showed that individual hydroxyl groups need to be separated from one another. When they are located close together, the hydroxyl groups dimerize and form a hydrogen bond, which cancels the dipoles and increases the energy required to dissociate the bond and to polarize the hydroxyl groups. It is, therefore, highly desirable to create a structure which is an alternate copolymer containing spacer groups, such as an ethylene unit, between each functional group.

Polarization-depolarization curves of hydroxylated polymers showed increases in the slopes, which indicate that more charges were stored on the surfaces of the dielectric film per unit voltage applied. At room temperature, the energy loss was minimal when a film was placed under a low electric field, such as 50 MV/m, yet the loss became larger with an increasing applied field.

The linear change of the slopes and irreversibility of the curves can perhaps be attributed to the induced and forced-dipolar polarizations. The tested temperature, room temperature, was below the T_g of the examined samples. During the polarization measurement, the amount of energy supplied to the samples could become important, allowing the hydroxyl group to become responsive when a sufficiently high electric field was applied. In other words, under a higher applied electric field, the hydroxyl groups were more poled, but the polarized hydroxyl groups did not get a chance to return to the original random state, which resulted in increased energy loss. For further investigation of the polarization curves, it is crucial to improve the film quality.

4.2 Suggestion for Future Work

4.2.1 One-pot Synthesis of Long Chain Branched Structure with PE Backbone and PP Branches

A two-step synthesis of long chain branched polymers containing a PE backbone and PP branches was introduced in Chapter 2. This approach maximized the BSt consumption and solubility of the polymer backbone. While it also allowed the custom-tailoring of the PE-BSt backbone structure, development of a one-pot synthesis would be much more convenient. In order to carry out the reactions in a one-pot scheme, the following key issues need to be solved: minimization of the molecular weight of PE-BSt to allow the subsequent reaction at lower temperature, optimization of the amount of solvent used to suit the reactions with ethylene and propylene, and enhancement of chain transfer to the styrene groups in PE-BSt. Among these

issues, tuning of the solvent quantity may be the most difficult problem. In a copolymerization of low-pressure ethylene and BSt, the use of large quantities of solvent reduces the catalyst reactivity and stability. In the reaction with propylene, however, large quantities of solvent are needed to keep PE-BSt in solution. It is possible to introduce extra solvent during the second step without opening the reactor. However, it would be ideal if the complication of solvent addition could be omitted from the reaction steps.

4.2.2 Hydroxylation of Non-polar Polymers

4.2.2.1 Structural Effect on the Dielectric Constant of a Functionalized Polyolefin

Various hydroxylated polymers were studied. The experimental results indicate that the mobility of the functional group was important. It is thus crucial to optimize the polymer structure. Two structures are suggested for a comparative study: hydroxylated 1,2-polybutadiene and a hydroxylated random copolymer of 1,2 and 1,4-polybutadiene.

As previously observed in the comparison of PP-OH 3 and PB-OH 50 in Chapter 3, attachment of a hydroxyl group at the end of butyl side chains helped to obtain a relatively high dielectric constant. Compared to highly hydrolyzed polyvinyl alcohol, 1,4-polybutadiene has a preferred structure due to the spacer groups between each hydroxyl groups. It is of interest to adopt these two advantages and to assess the dielectric properties of the material. A hydroxylated 1,2-polybutadiene and a random copolymer of 1,2 and 1,4-polybutadiene may exhibit improved dielectric properties compared to 1,4-polybutadiene.

4.2.2.2 Film Stability and Polarization Curves of Hydroxylated Polymers

Polarization studies of hydroxylated polymers exhibited the potential benefits of functionalization. Room temperature studies of polarization loops showed an increase in the slopes. At elevated temperatures, such as 50 °C, the films were unstable, and reduced breakdown strength and irreversibility of the polarization curve were observed. For better performance at high temperatures, thermal stabilization of the film is crucial. One proposed route to improve the thermal stability of a film is through crosslinking. Schneuwly reported a reduction in the breakdown strength of polypropylene films at elevated temperatures and attributed it to movement of polymer chains.¹ Crosslinking of the polymer backbone, therefore, is expected to give better thermal stability. No immediate negative effect is expected from partial or light crosslinking, as the hydroxyl group remains mobile and can be polarized.

4.2.2.3 Functionalization with Other Polar Groups

Dielectric constants of non-polar polymers were improved using a hydroxyl group functionalization. One of the advantages of this system over a fluoropolymer-based system was its structure, where only the functionalized groups responded to the electric field. In the case of a fluoropolymer, such as p(VDF-TrFE-CFE) terpolymer, the polymer chains also go through a crystal orientation. As a result, detailed tuning of the crystal structures is needed to improve the reversibility of the film under an electric field. Reversibility is also important in a functionalized non-polar polymer, yet one reduced factor may make it easier to optimize its structure. As previously mentioned in Chapter 3, the dipole moment of a hydroxyl group is about 1.6, which is relatively close to that of PVDF, 2.1. It is of interest to adopt a polar group with greater polarity for a new capacitor material with improved dielectric properties.

References

1. Schneuwly, A.; Groning, P.; Schlapbach, L.; Irrgang, C.; Vogt, J., Breakdown behavior of oil-impregnated polypropylene as dielectric in film capacitors. *Dielectrics and Electrical Insulation, IEEE Transactions on* **1998**, 5, (6), 862-868.